

Field and method course - Greenland

Maja la Cour Bohr (pdn810), Peter Bo Mähl (fjx197), Stinna Susgaard

Filsø (bwk750), Søren Pierre Aagaard (hnf440)

Active Layer Modelling



Vejleder: Birger Ulf Hansen

Institut for Geovidenskab og Naturforvaltning

Submitted: 28th of October 2015

Contents

1	Foreword	2
2	Introduction	4
2.1	Permafrost in the context of climate warming.....	4
2.2	Factors controlling the active layer thickness.....	4
2.3	Stefan Solution	5
2.4	Study area description: Disko Island.....	6
2.4.1	Geology	6
2.4.2	Climatology of Disko Island	6
2.4.3	Bioclimatic zones and vegetation	9
2.5	Study site description: Transect A, B, C.....	10
3	References	12

Paper 1: Estimating NDVI and nt-factor on Disko Island, Greenland, using different in situ methods pp. 1-14

Paper 2: The Impact of Different Incorporated Factors in Active Layer Thickness Modelling using Stefan Solution pp. 1-14.

Appendix: Field schedule

1 Foreword

The Department of Geoscience and Natural Resource Management and the Faculty of Sciences at University of Copenhagen continue to emphasize the importance of conducting a field course in Arctic Physical Geography at Arctic Station, Qeqertarsuaq (Godhavn), Disko Island, West Greenland. Hence, every fourth year this course enables a selected group of students enrolled at University of Copenhagen to perform their own research projects in close collaboration with a supervisor.

The 2015 course was out of this four year cycle, so it was held as a project course outside the course scope with a physical geography part and a biological part. This report covers the physical geography part.

The projects are carefully prepared and the planning started five months in advance to the beginning of the field course. The field course provides for the first time the possibility to experience the Arctic environment in a three-dimensional space. Furthermore, the practical projects deliver a significant hands-on experience that not even the best textbook will be able to encompass. With the persistent national and international interest in the Arctic environment and the numerous ongoing studies addressing the effects of global warming on the Arctic climate, it is of outmost importance that students for years to come are given the opportunity to do research and learn about the Arctic in general.

The Field Course in Physical Geography 2015 took place between the 1-12th of August at Disko in West Greenland. Four students (Stinna Susgaard Filsø, Maja la Cour Bohr, Søren Pierre Aagaard and Peter Bo Mähl) participated in the physical geography part of the course and five students (Frederikke Høyier, Simone Gress Hansen, Marie Richter Flyger, Emilie Thane Christensen and Nikolaj Lundsgaard Kindtler) participated in the biological part of the course. They have now completed the different parts: Preparations i.e., fine-tuning of projects, packing of equipment and the actual field course in Greenland. This report represents the final results for the physical geography part of the course. The course was organized and lead by Birger Ulf Hansen and Ole Humlum.

The aim of the Field Course in Physical Geography 2015 was to investigate:

1. Estimating NDVI and nt-factor on Disko Island, Greenland, using different in situ methods
2. The Impact of Different Incorporated Factors in Active Layer Thickness Modelling using Stefan Solution

The combination of these two parts can provide new insight with respect to the current and future permafrost thawing within the study area taken current and future climate trends into account. The southern part of "Blæsedalen" was chosen as the study area due to the fact that the landscape is fairly well-described and due to the presence of all landscape types representative for the Arctic environment.

Part of the course has been directly linked to CENPERM – a center of excellence, which will integrate hypothesis-based studies of biogeochemical and physical processes in a "climate-vegetation-soil-microorganism-permafrost" context. Therefore, several other people took part in the field work at Disko this summer including Bo Elberling, Per Ambus, Mojtaba Karami, Andreas Westergaard-Nielsen, Guy Schurgers, Paul Christiansen, Bente Gade, Anders Michelsen, Karsten Høgh Jensen, Sebastian F. Zastruzny, Tue Mariager, Michelle Cruz Riis, Lisbeth Simonsen.

Thanks to 4 enthusiastic students, the CENPERM Center, Arctic Station (including Christian Juncker Jørgensen, Gitte Henriksen, Kjeld Akaaraq Mølgaard) as well as Faculty of Science, University of Copenhagen for financial supporting this Field Course in Physical Geography.

October 2015

Birger Hansen
(Course responsible)



Stående fra venstre: Paul Christiansen, Mette Sinding Francke, Bo Elberling, Kjeld, Akaaraq Mølgaard, Andreas Westergaard Nielsen, Karsten Høgh Jensen, Sebastian F. Zastruzny, Tue Mariager, Søren Pierre Aagaard, Ole Humlum, Nikolaj Lunding Kindtler, Birger Ulf Hansen, Anders Michelsen, Mojtaba Karami

Siddende fra venstre: Bente Marie Gade, Frederikke Hoyer, Simone Gress Hansen, Marie Richter Flyger, Stinna Susgaard Filsø, Maja La Cour Bohr, Michelle Cruz Riis, Emilie Thane Christensen, Peter Bo Mähl, Guillaume J.J.A. Schurgers, Lisbeth Simonsen.

2 Introduction

2.1 Permafrost in the context of climate warming

Warming of the climate system is evident, affecting the climate globally (IPCC, 2014). This warming is not evenly distributed throughout the globe and the Arctic region experiences temperature rises exceeding the global average (Carlowicz, 2014). The amplified temperature rise in the Arctic is primarily caused by positive feedbacks, such as melting of sea ice and inland ice leading to decreased surface albedo and thus increased surface temperature and thawing of frozen ground. This releases otherwise sequestered carbon back to the atmosphere and further induce the temperature rise (Bonan, 2008) (Hollesen, et al., 2011). In this regard, monitoring and modelling frozen ground, also known as permafrost, have been widely used in climate change research. Permafrost is an important parameter due to its sensibility to changes in surface temperatures and other climatic parameters as well as its influence on the global climate system through alterations in energy exchanges, hydrological processes and carbon budgets (Riseborough, et al., 2008).

Permafrost is defined as “*earth material that remains continuously at or below 0 °C for at least two consecutive years*” (Bockheim, 2015). The near surface layer of permafrost is subject to thaw in the summer and refreezing in the winter and is referred to as the active layer (Bockheim, 2015). The active layer is important because the majority of the ecosystem and hydrological processes in permafrost areas occur within this layer, and thawing is associated with potentially releasing large quantities of carbon to the atmosphere (Bonnadventure & Lamoureux, 2013). The warming of the climate is expected to be reflected in increased active layer thicknesses, leading to further increase in air temperature (Hollesen, et al., 2011). On this matter, the thickness of the active layer is essential as a larger thawing depth takes longer to refreeze in the autumn and thereby has the potential of a greater carbon mineralization and release (Hollesen, et al., 2011).

2.2 Factors controlling the active layer thickness

The overall existence of permafrost and the thickness of the active layer are governed by soil temperature which is a product of heat exchange between the atmosphere and the ground surface (Zhang, et al., 1997) (Hollesen, et al., 2011). Factors that affect the surface heat balance would also influence the active layer thickness (Zhang, et al., 1997). The different factors are often closely interrelated and can be seen as a combination of several macro- and micro variables. The broadest controls on active layer thicknesses are influences that govern the surface climate such as: solar insolation patterns, albedo, latitude, elevation and proximity to glaciers and water bodies (Bonnadventure & Lamoureux, 2013). However, where these macro variables causes the mean annual temperature to be within a few degrees of 0 °C, local variations in surface conditions determine the spatial distribution of active layer thicknesses within the area based on differences in the ground thermal regime (Street & Melnikov, 1990).

Important local factors that influence surface energy balance and hence the ground thermal regime, are snow cover, vegetation, and soil. When precipitation falls as snow, it can accumulate and form a snow cover which due to its low thermal conductivity, can provide insulation to the ground (Street & Melnikov, 1990). Warmer ground conditions require less energy to thaw in the melt season (Bonnadventure & Lamoureux, 2013). The depth of snow cover is a product of amount of precipitation, temperature, wind patterns, ground surface morphology, and vegetation, whereas the insulating effect of snow is depended on the density, structure and thermal properties of the seasonally snow cover (Zhang, et al., 1997). Besides the snow cover depth, the timing of the snow cover formation and melt is also crucial for the ground thermal regime. Early snow fall results in less freezing of the ground due to the insulation (Street & Melnikov, 1990). Snow cover would act as a heat sink during the spring, and insulating as well as reflecting the incoming solar radiation, thereby reducing the thawing of the active layer (Zhang, et al., 1997).

Vegetation also acts as an insulating buffer between the atmosphere and the soil. Vegetation cover is mainly controlled by climate and soil type, but the presence of permafrost has an influence. The active layer is a nutrient source and a shallow active layer maintains water and nutrients close to the surface (Street & Melnikov, 1990). However, a shallow active layer can also restrict vegetation growth as permafrost is relatively impermeable and acts as a barrier to root growth and to the movement of water, which can cause saturated conditions in the root zone. The low soil temperatures also reduce the nutrient availability and the rate of decomposition that leads to the formation of an organic layer (Street & Melnikov, 1990).

Vegetation influences the active layer thickness in two ways. Vegetation canopy reduces the amount of solar radiation reaching the ground and inception and transpiration alter the ground thermal regime through evaporation and variations in the water balance (Street & Melnikov, 1990). Additionally, vegetation influences accumulation and persistence of snow cover which again affects the vegetation cover as snow cover both protect the vegetation from the winter frost as well as reduce the amount of energy available for plant growth in spring and early summer (Street & Melnikov, 1990). The presence of vegetation can further result in formation of an organic layer on top of the mineral soil. Such an organic layer consists of undecomposed organic material, usually peat, and provides insulation against summer thaw and increase soil moisture (Street & Melnikov, 1990). Due to a low thermal conductivity when wet, the organic layer inhibits warming of the soil in summer. In the winter, as the water in the organic layer freezes, thermal conductivity increases enhancing the cooling of the ground (Bonnnaventure & Lamoureux, 2013). This variation in thermal conductivity results in a cooler mean ground thermal regime under an organic layer compared to the surrounding areas without one, and can even for extended time periods sustain permafrost when temperatures are slightly above 0 °C (Bonnnaventure & Lamoureux, 2013). Street & Melnikov (1990) mention how vegetation cover has only a minor influence on the soil thermal regime compared to the existing of an organic surface layer

and that the presence of sporadic and discontinuous permafrost is commonly associated with such a layer.

Soil is another site-specific factor that influences the thickness of the active layer. The physical properties of soil such as texture, structure, and bulk density determine the drainage capacity (and hence the soil water content), nutrient availability, gas fluxes, and soil temperature (Bockheim, 2015). Soil temperature is determined by the soils ability to conduct and store heat (Bonan, 2008). Thermal conductivity and heat capacity variation highly depends on the physical properties of the soil as well as the organic matter content and soil moisture content. The soil water content also affect how much of the incoming energy to the soil goes to freeze and melt the water, which again affect the soil temperature and thus the thickness of the active layer (Barry & Gan, 2012). Furthermore, wet soils have a higher evaporation, which cools the surface and reduce ground temperature (Bonan, 2008).

2.3 Stefan Solution

The thickness of the active layer and characteristics of permafrost can act as an indicator of climate change happening in the Arctic region. For this reason, estimating the active layer thickness has been of great interest. Two approaches of estimating the thickness exist; either directly by monitoring permafrost areas using methods such as mechanical probing, measurements of soil temperatures or visual observations, or indirectly via modelling (Zhang, et al., 2005).

A model is a conceptual or mathematical representation of a phenomenon, and modelling of the active layer thickness have been applied in several cases in order to investigate the effects of climate change on Arctic regions (Zhang, et al., 2005) (Nelson & Outcalt, 1987). Numerous parameters influence the behavior of the active layer. Air and surface temperature, duration of thawing season, snow cover, substrate heterogeneity, vegetation, topoclimate, and soil thermal properties are some. An ideal model of permafrost predictions includes the above-mentioned macro- and microclimatic parameters because both variables are interrelated

(Nelson, 1986) (Anisimov, et al., 1997). For this reason, the most widely employed equation in active layer modelling is the Stefan solution or its modifications (Riseborough, et al., 2008).

The depth of the active layer (Z) can be estimated based on a modified Stefan solution derived from Zhang et al. (2005):

$$Z = E * \sqrt{n_t * PRI * DDT} \quad \text{Equation 1}$$

In this equation, E is a measure of the edaphic factor, PRI is the potential radiation index, DDT is degree-days of thaw and n_t equals the n-factor of thaw ($= T_s/T_a$). The modified Stefan equation is composed of an edaphic term (E) and a climatic term (n_t , PRI , DDT) (Nelson & Outcalt, 1987).

2.4 Study area description: Disko Island

Active layer modelling and investigation of different in situ NDVI methods for vegetation monitoring are conducted around Arctic Station ($69^{\circ}15'N$, $53^{\circ}31'W$) build in 1906 by M.P Porsild. Arctic Station is located on Disko Island (8600 km^2) in West Greenland near the Greenlandic settlement Qeqertarsuaq outside the coast of the mainland of Greenland (see Figure 1) (Humlum, 1998) (Hansen, et al., 2006a).

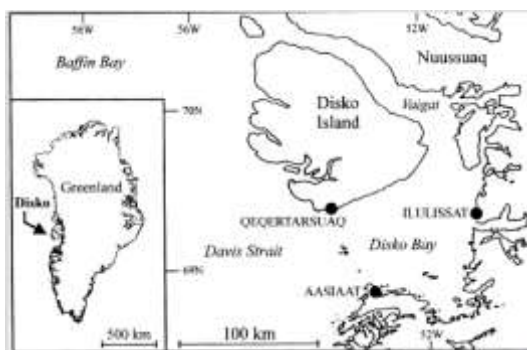


Figure 1: Location of Qeqertarsuaq, Disko Island (Humlum, 1998).

2.4.1 Geology

The landscape around Arctic Station is part of a low bench of gneiss – however, the main landscape of Disko Island consists of a Tertiary breccia volcanic province of West Greenland and is composed mainly of plateau lavas (Humlum, 1998) (Hansen, et al., 2006a). The Tertiary breccia reaches a total depth of 5000 m (Humlum, 1996). A typical Arctic is domi-

nated by a plateau basalt landscape with deeply incised Quaternary cold-climate landforms such as cirques, trough valleys and fjords (Humlum, 1998). Steep mountain slopes from the south-western part of the island to the north-eastern part raise the terrain significantly from 800 m a.s.l. in the SW to more than 1900 m a.s.l. in the NE (Humlum, 1998).

2.4.2 Climatology of Disko Island

The primary controllers of the climate of Greenland are the inland ice sheet – covering 80% of the total Greenland area and the collision of cold winds coming from north/northwest and warm winds coming from south (Hansen, et al., 2006b). The climate of Disko Island and the study area is influenced by additional factors such as dissemination of winter and summer sea ice and sea currents.

In the following sections, the local climate on Disko Island is based on meteorological data from climate stations during the period 1991-2015. Parameters to estimate meteorological trends include daily observations of snow cover, sea ice cover and bihourly logged air, precipitation and solar radiation (Hansen, et al., 2006a).

Solar radiation and albedo

This northern location of Disko Island (latitude $69^{\circ}15'$ N i.e. north of the Arctic Circle) has a fundamental effect on the incoming shortwave radiation as sun angle in general is very low at high latitudes. The annual variation in incoming- and outgoing radiation for the study area is shown in figure 2 on the next page which is based on data from a period of 1991-2004 made available from the meteorological station at Arctic Station, where all sensors have logged data with a 30 minutes scanning frequency (Humlum, 1996).

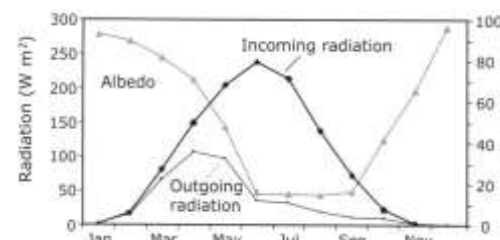


Figure 2: Mean monthly incoming and outgoing solar radiation and albedo at the Arctic Station (1991-2004) (Hansen, et al., 2006a).

Annual variation is very distinct for incoming solar radiation and albedo. The incoming solar radiation is highest in the summer months and very low in the winter, where the sun does not appear above the horizon from November 29th to January 11th. The albedo however, is highest in the winter and lowest during summer as a function of snow cover.

The annual variation in incoming- and outgoing radiation is also amplified by cloud cover and local variation such as terrain orientation (shade from mountains), slope, and snow cover (Hansen, et al., 2006b). Incoming solar radiation is reduced with a thick cloud cover. In years with a deep snow cover, the incoming solar radiation is used to snow melt instead of plant production. In those years, the growing season is postponed and thereby reduced.

Sea Ice

The sea ice along the coast of Greenland is a central climate factor because solar radiation is reflected by the high albedo from sea ice. This creates high pressure conditions as the reflected solar radiation results in a cooling of the atmospheric layers near the surface (Hansen, et al., 2006a). High pressure is associated with relatively stable air conditions, thus years with no sea ice would be associated with more unstable low pressure situations.

Local sea ice coverage around Disko Island is observed daily near Arctic Station. The total sea ice coverage from 1991-2015 around Disko Island, Vestisen, is presented in Figure 3 and shows the annual variations. The extent of Vestisen is observed from January to April/May. From 1991-2004 the sea ice in the Disko bay have been reduced by approximately 50 % (Hansen, et al., 2006b) and the trend seems to continue for the following years. This decreasing trend is seen in both ends of the season and even a total absence (roughly) of sea ice is observed in 2010. A decrease in sea ice extent represents a heat input as less solar radiation is reflected (Hansen, et al., 2006b). However, in later parts of the period, a reappearance of years with more sea ice is seen (for the years 2008, 2009, 2012, 2013, and 2015) suggesting a greater proportion of the year with stable air parcels and colder weather conditions.

Air temperature

According to Humlum (1998), air temperature generally represents the major control on active layer temperatures at Qeqertarsuaq. From the continuous 1991-2015 data series of annual air temperatures shown in Figure 4 on the next page, it can be seen that these vary inter-annually.

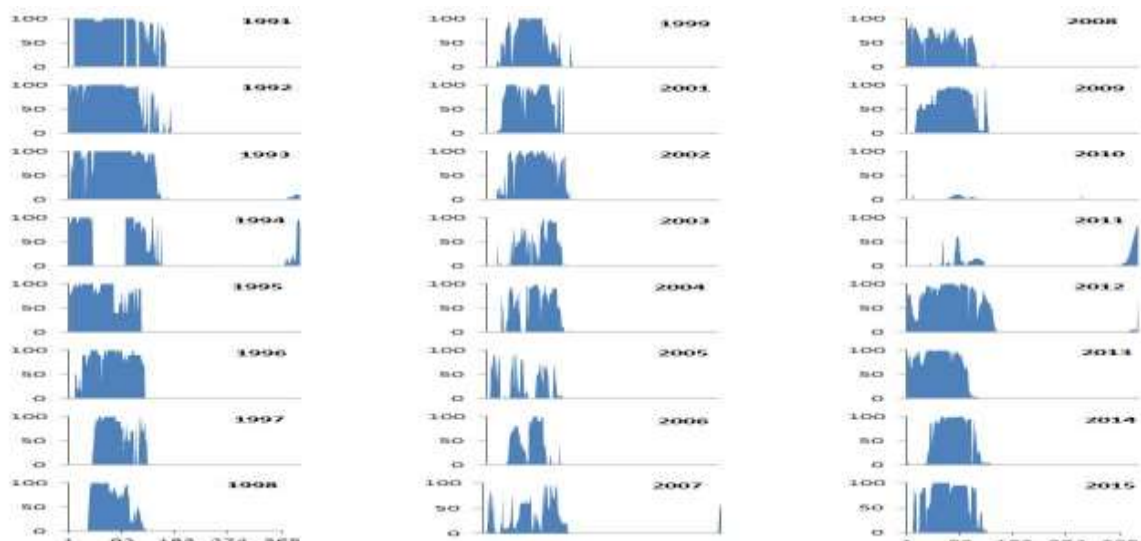


Figure 3: Daily sea ice observations in the year 1991-2015 at Arctic Station. The unit of the vertical axis is percentage. Year 2000 has missing sea ice data and data during the spring of 1994 is missing as well.

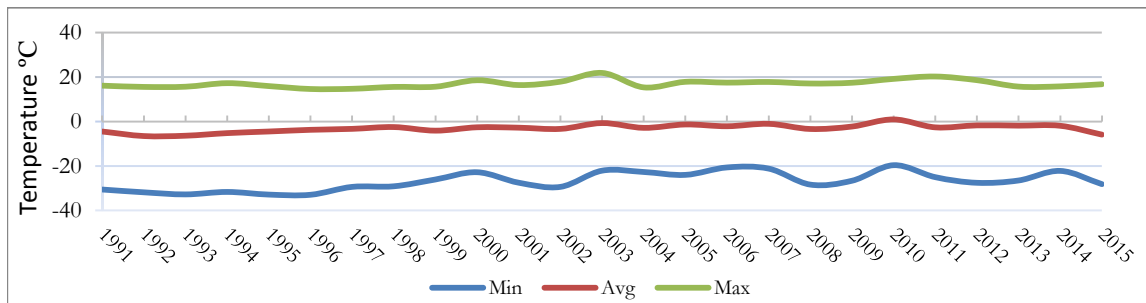


Figure 4: Annual minimum, average and maximum air temperatures measured over a period of 1991-2015. The measured air temperatures were measured 10 m above terrain (and not at 2 m, which is normal practice) with a 30 min interval.

An increase in annual average air temperature from 1991-2015 can be detected, an increase primarily caused by an increase in average minimum air temperatures.

Besides for variation between years, the air temperature also varies significantly within a year. Variation in air temperature with monthly mean, minimum and maximum is based on data from 1991-2015 and is presented in Figure 5.

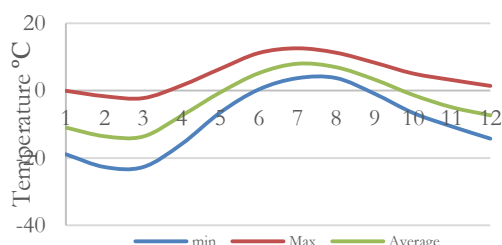


Figure 5: A monthly minimum, average and maximum air temperatures – 1991-2015

July is on average the warmest month with a mean air temperature of 8.0 °C and the coldest month is March with a mean air temperature of -13.65 °C. There is a larger difference in air temperature between maximum and minimum values in the colder months of January-March than the rest of the year. This indicates the inter-annual variation of air temperature is greater in the winter months than in the summer months.

2.4.2.1 Precipitation

Mean annual precipitation at Arctic Station is about 400 mm where 60-70% falls as snow (Humlum, 1998). Precipitation in Greenland is associated with low pressure systems from west passing a large elevation gradient from the coast towards the ice cap (Hansen, et al., 2006b). In the period of June-

December, 75% of precipitation is related to the advection of moist, maritime air masses from the south and southwest along the Davis Strait (Humlum, 1998). The rest of the year, dry and cold continental polar fronts from the ice cap are flowing towards east.

The amount of precipitation at Arctic Station in 2015 (till the 15th of August) was measured at 62.4 mm.

Snow cover

Snow cover observations at Arctic Station have been measured in the period 1991-2015 (figure 6 on the next page).

The snow cover depths vary very much from year to year. This could result in similar variation in the active layer thickness as these are controlled by snow cover and its effect on the soil thermal regime (Bonnaveutre & Lamoureux, 2013).

The 24-year period indicates a decrease in the annual duration of the snow cover with a trend showing an earlier snow-free surface date and a decrease in the annual volume of snow. Noticeably is the observed change in snow cover during the last 9 years (2005-2014), where snow depths above 30 cm have not been observed. Periods with a low snow cover have been observed before in 1994, 1995, 1997, 2002, and 2003. However, 2015 seems to be a turning point for the decreasing annual snow cover, with deeper snow cover in the beginning of the year than for previous years.

As mentioned earlier, snow cover can provide insulation to the ground and thereby influence the active layer thickness. The decreasing trend in snow cover volume and duration at Disko is therefore a relevant

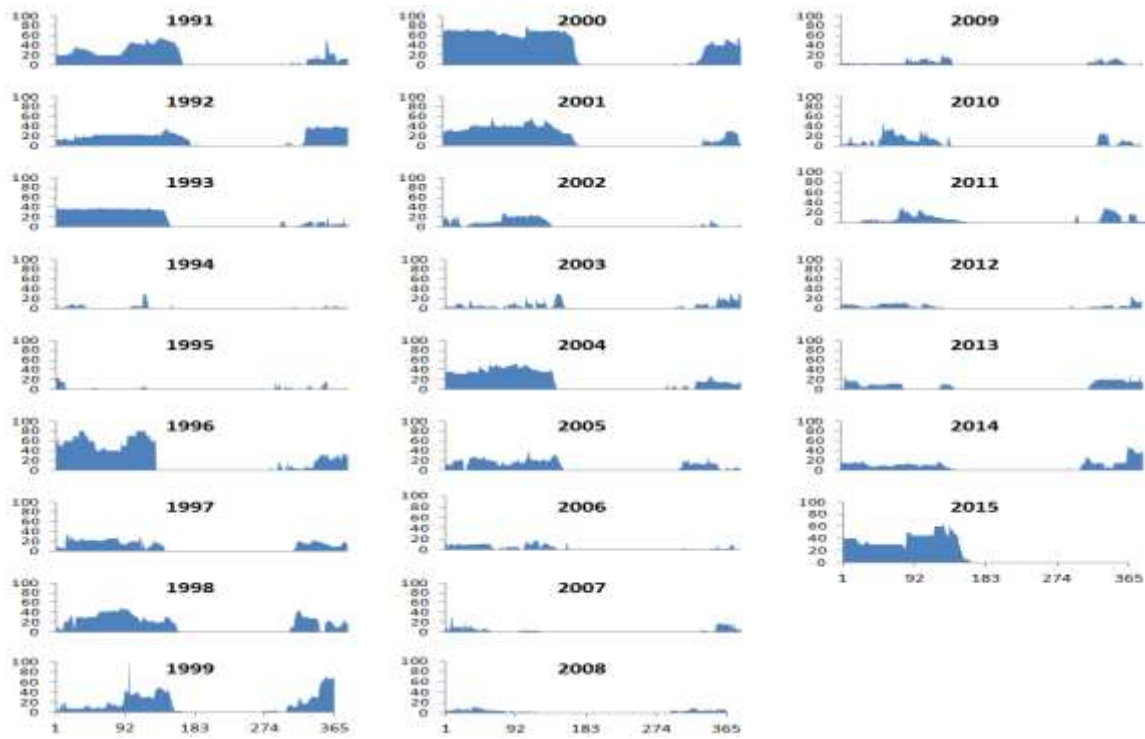


Figure 6: Daily snow depth observations in year 1991-2015 at Arctic Station. The unit of the vertical axis is centimetre

factor to consider when estimating future active layer thickness

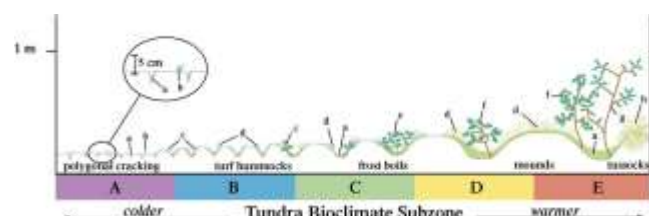
2.4.3 Bioclimatic zones and vegetation

The Arctic climate zone is characterized by having a temperature below 10 °C in the warmest month. Disko Island is located between high and low Arctic, the high Arctic zone having summer temperature < 5 °C and the low Arctic zone summer temperatures between 5-10 °C (Hansen, et al., 2006b).

The arctic zone has been further divided into bioclimatic subzones from A-E, mainly based on difference in summer temperature and vegetation (Walker, et al., 2005). Figure 7 presents features of the different subzones.

The vegetation on Disko Island is very diverse compared to other locations on the same latitude, i.e. due to a location in a transition zone between high and low Arctic. Thus, 70 % of all plant species in West Greenland are to be found at Disko (Mølgaard, et al., 2006).

A short growing season and cold temperatures leads to low, robust plant species (Mølgaard, et al., 2006). Furthermore, certain areas are influenced by cryoturbation, affecting vegetation cover. Cover fraction analysis identified crowberries, dwarf birch, willow, bog bilberry and horsetail as some of the most dominant plant species in and around Blæsedalen. Also different species of moss were common. Table 1 on the next page presents the most dominant species at the investigated areas.



Sub-zone	Definition	SWI	T _a mean, July °C
A	Arctic Polar Desert	<6	0 – 3
B	Northern Arctic Tundra	6-9	3 – 5
C	Middle Arctic Tundra	9-12	7 – 9
D	Southern Arctic Tundra	12-20	9 – 11
E	Arctic Shrub Tundra	20-35	11 – 13

Figur 7: Bioclimatic subzones A-E. SWI is summer Warmth Index. Subzone A has coolest temperatures and most barren ground whereas subzone E is the warmest and most vegetated. From Walker et al. (2005)

Table 1: Dominant plant species in and around Blæsedalen

Crowberries (*Empetrum hermaphroditum*) is a dwarf shrub at 3-20 cm height, dominating in Blæsedalen.

Bog bilberry (*Vaccinium uliginosum*) is common in heaths and bogs in most of Greenland, up to 79 °N.

Dwarf Birch (*Betula nana*) can be up to 100 cm tall, is common on heaths, in fell-field and bogs and was often observed in Blæsedalen, though only in up to 20 cm tall.

Willow (*Salix glauca*) is common on especially wet areas. Willow is one of the tallest vegetation species on Disko and was observed up to 100 cm.

Horsetail (*Equisetum arvense*) grows on moist, clayey soil. The roots tolerate cryoturbation and the plant can therefore be a sign of permafrost.

Source: (Rune, 2011)

The amount of green, healthy vegetation within a specific spatial unit can be analysed via The Normalized Difference Vegetation Index (NDVI). In the Arctic, NDVI can be an indicator of vegetation cover fraction, as arctic plant species typical growth in width instead of height. Furthermore, larger NDVI is associated with higher amount of different plant species, ranging up to communities with 500 species in subzone E (Mølgaard, et al., 2006). Walker et al. (2006) related NDVI to biomass using clip harvest data, and found that both NDVI and biomass increased from north to south (subzone A-E). Thus, NDVI is related to temperature and therefore highly sensitive to climatic changes and change in climate zones. The response of NDVI on changing climatic conditions makes NDVI a useful index to assess changes in climate. Especially for subzone A, temperature is the controlling factor for vegetation since plants are constrained by the cold climate. For subzone B-E, other factors such as elevation, moisture, substrate availability and geomorphology also impact vegetation and thus NDVI.

2.5 Study site description: Transect A, B, C

The investigations conducted for this report are all more or less centred about calculating the active layer thickness of three transects. These represent three different locations with different vegetation characteristics. As the spatial distribution of active layer thickness is dependent on vegetation cover and soil wetness, these parameters were incorporated in the selection criteria of sites. First of all,

sites were chosen based on a difference in vegetation between locations and a vegetation gradient within each location. Furthermore, the locations should also differ in wetness. Wetness is often seen to correlate with vegetation, as it is a controller on vegetation growth. Similarity in topography, such as slope and aspect, was the last criterion in order to eliminate the influence of PRI.

A two-step process was conducted to locate the transects. Initially, a NDVI map was created where preliminary calculations of NDVI from satellite data (Landsat 4-5 & 8) divided Blæsedalen and adjacent areas into 7 NDVI classes (see figure 14 in paper *'Estimating NDVI and nt-factor on Disko Island, Greenland, using different in situ methods'* for map over vegetation classes). Based on this map, three areas with different NDVI classes were detected.



Figure 8: Shows the areas under investigations in this report. The spatial distribution of the three transects and the used climates stations both fixed and mobile. Image is a World View 2, 2012.

When potential areas were identified, they were reviewed in situ before finally confirmed. The locations selected are presented in figure 8 on the previous page.

Transect A represents a location with a lot of vegetation and an intermediate wetness condition and is situated in Østerlien. Transect B constitutes an abrasion plateau with very sparse vegetation and fairly dry wetness conditions, located at the mouth of Blæsedalen. Transect C is located in Blæsedalen at the foot of Pjetursson's Moraine next to a lake and represents a location highly vegetated and saturated. Figure 9 shows photos of the three transects.

Table 2 presents a further description of the transects in regard to dominant vegetation types, water content, and soil texture. As seen, the three transects vary for all categories.

Table 2 Transect descriptions

	Dominant vegetation type	Average water content	Texture
Transect A	Vaccinium, <i>Salix glauca</i>	76 %	Silty loam and sandy loam
Transect B	Vaccinium, <i>Betula nana</i> , plant litter, bare soil	18 %	Sand
Transect C	Moss, Horsetail, <i>Salix glauca</i>	101 %	Silt and silty loam

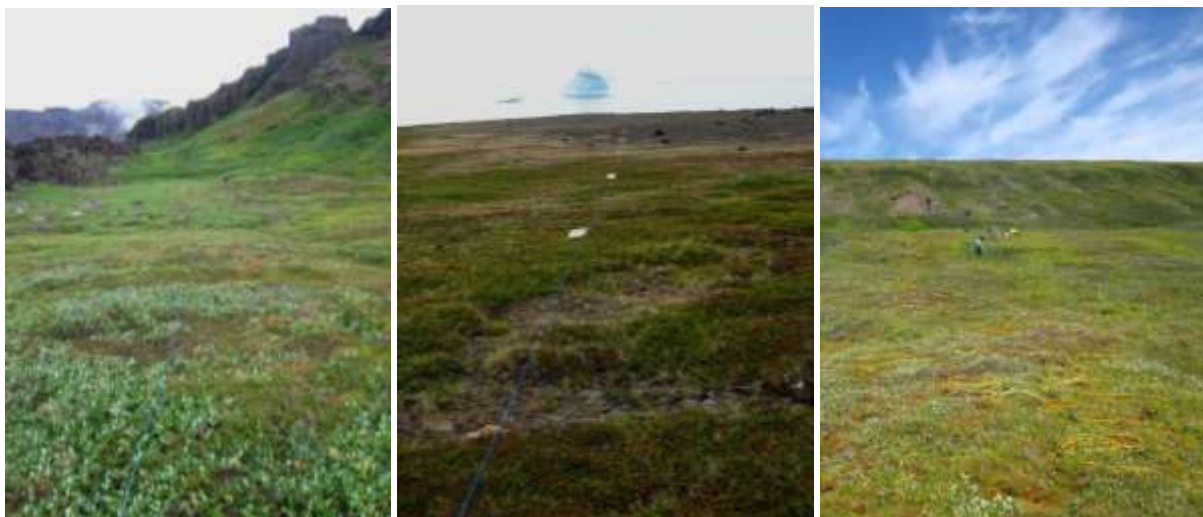


Figure 9: Transect A in Blæsedalen. Transect B at the mouth of Blæsedalen. Transect C in Blæsedalen near the lake. Transect A and C are photographed towards North whereas the photo of Transect B is directed towards South. Private photos.

3 References

- Anisimov, O. A., Shiklomanov, N. I. & Nelson, F. E., 1997. Global warming and active-layer thickness: results from transient general circulation models. *Global and Planetary Change*, Volume 15, pp. 61-77.
- Barry, R. & Gan, T. Y., 2012. Frozen ground and permafrost. In: R. Barry & T. Y. Gan, eds. *The Global Cryosphere*. Cambridge: Cambridge University Press, pp. 165-189.
- Bockheim, J. G., 2015. *Cryopedology*. Switzerland: Springer.
- Bonan, G., 2008. *Ecological Climatology - Concepts and Applications*. 2. ed. New York: Cambridge University Press.
- Bonnadventure, P. P. & Lamoureux, S. F., 2013. The active layer: A conceptual review of monitoring, modelling techniques and changes in a warming climate. *Progress in Physical Geography*, 37(3), pp. 352-376.
- Carlowicz, M., 2014. *Global Temperatures*. [Online] Available at: <http://earthobservatory.nasa.gov/Features/WorldOfChange/decadaltemp.php> [Accessed 16. 09. 2015].
- Hansen, B. U., Elberling, B., Humlum, O. & Nielsen, N., 2006a. Meteorological trends (1991-2004) at Arctic Station, Central West Greenland ($69^{\circ}15'N$) in a 130 years perspective. *Geografisk Tidsskrift-Danish Journal of Geography*, 106(1), pp. 45-55.
- Hansen, B. U., Elberling, B., Nielsen, N. & Hollesen, J., 2006b. Vejret og klimaet. In: L. Bruun, et al. eds. *Arktisk station 1906-2006*. Copenhagen: Arctic Station, University of Copenhagen, Forlaget Rhodos, pp. 44-57.
- Hollesen, J. ., Elberling, B. & Jansson, P. E., 2011. Future active layer dynamics and carbon dioxide production from thawing permafrost layers in Northeast Greenland. *Global Change Biology*, Issue 17, pp. 911-926.
- Humlum, O., 1996. *Origin of rock glaciers: observations from mellemfjord, Disko Island, Central west greenland*, s.l.: s.n.
- Humlum, O., 1998. Active Layer Thermal Regime 1991-1996 at Qeqertarsuaq, Disko Island, Central West Greenland. *Arctic and Alpine Research*, 30(3), pp. 295-305.
- IPCC, 2014. *Summary for Policymakers*, s.l.: IPCC.
- Mølgård, P., Christiansen, A. & Pedersen, P. M., 2006. 1.05 Plantelivet. In: *Arktisk Station 1906-2006*. København: Arktisk Station - Københavns Universitet, pp. 70-83.
- Nelson, F. E., 1986. Permafrost Distribution in Central Canada: Applications of a Climate-Based Predictive Model. *Annals of the Association of American Geographers*, 76(4), pp. 550-569.
- Nelson, F. E. & Outcalt, S. I., 1987. A Computational Method for Prediction and Regionalization of Permafrost. *Arctic and Alpine Research*, 19(3), pp. 279-288.
- Riseborough, D. et al., 2008. Recent Advances in Permafrost Modelling. *PERMAFROST AND PERIGLACIAL PROCESSES*, Issue 19, pp. 137-156.
- Rune, F., 2011. *Wild Flowers of Greenland*. Flemming Rune ed. Hillerød: 15. Juni Fonden, Kulturfonden Danmark-Grønland, Aase og Jørgen Münthers Fond.
- Street, R. B. & Melnikov, P. I., 1990. Seasonal snow cover, ice and permafrost. In: W. M. Tegart, G. Sheldon & D. Griffiths, eds. *Climate Change: The IPCC Impacts Assessment*. Canberra: IPCC, pp. 257-293.
- Walker, D. A., Raynolds, M. K., Fred, J. & Einarsson, E., 2005. The Circumpolar Arctic vegetation map. *Journal of Vegetation Science* 16, pp. 267-282.
- Walker, D., Raynolds, M. & Maier, H. A., 2006. NDVI patterns and phytomass distribution in the

circumpolar Arctic. *Remote Sensing of Environment* 102, p. 271–281.

Zhang, T. et al., 2005. Spatial and temporal variability in active layer thickness over the Russian Arctic drainage basin. *JOURNAL OF GEOPHYSICAL RESEARCH*, Volume 110, p. D16101.

Zhang, T., Osterkamp, T. & Sturm, K., 1997. Effects of Climate on the Active Layer and Permafrost on the North Slope of Alaska, U.S.A.. *Permafrost and Periglacial Processes*, Issue 8, pp. 45-67.

Estimating NDVI and nt-factor on Disko Island, Greenland, using different in situ methods

Maja la Cour Bohr¹, Peter Bo Mähl¹, Stinna Susgaard Filsø¹, Søren Pierre Aagaard¹

¹Cand.Scient Stud, Geography and Geoinformatics, Department of Geosciences and Natural Resource Management, University of Copenhagen

Abstract

A Skye sensor, NDVI camera, and Decagon Sensor are evaluated with respect to application-accuracy for vegetation monitoring. Three transects are investigated A, B and C, as well as 35 additional points. Decagon sensor and NDVI camera showed a consistent relationship between NDVI values, and relative values from camera are converted to absolute NDVI values based on this. The Skye sensor showed no consistent results and is dismissed. Average NDVI are found to be 0.52, 0.29, and 0.49 for transect A, B, and C, respectively. NDVI obtained from Landsat 8 is generally lower than those obtained from in situ methods.

A relationship between NDVI and nt-factors is established from climate stations. From this, nt-factors have been estimated to be between 1.27-0.76. Mean nt-factors are 0.78, 0.90 and 0.80 for transect A, B and C, respectively. At transect B, nt-factors above 1 occurs, indicating higher surface than air temperatures. Correlation between NDVI and incoming solar radiation have been evaluated and show a bias in the NDVI result when the incoming solar radiation is below 100 W m^{-2} .

Key words: NDVI, nt-factor, vegetation monitoring, NDVI camera, Spectral Reflectance Sensors.

1 Introduction

The thaw depth of permafrost is dependent on the energy balance at the soil surface as it determines the amount of energy available for thawing the permafrost (Zhang, et al., 1997). The surface energy balance is a term describing how the net radiation absorbed by the ground is balanced by energy gained or lost by sensible heat, latent heat, and changes in heat storage (Bonan, 2008). The fraction of sensible heat, latent heat, and heat storage determines the amount of energy present at the ground surface. This balance varies geographically in relation to incoming solar radiation and soil water availability and thus vegetation (Bonan, 2008). Vegetation canopy reduces the amount of solar radiation reaching the ground. Canopy interception and transpiration alter the ground temperature through evaporation and variations in the water balance (Street & Melnikov, 1990). Furthermore, vegetation might act as an insulating cover, leading to slow thaw progression (Nelson et al. 1997).

The influence of vegetation on the active layer thickness is complex as it consists of compound interrelations, e.g. between surface temperature, plant growth, and a thermal insulating factor. This leads to large local variability in active layer thickness due to namely different vegetation cover and organic layer thickness (Zhang, et al., 1997) (Myneni, et al., 1997).

Due to its importance, the surface energy balance is included in modelling of the active layer thickness in terms of an n-factor (Riseborough, et al., 2008). The n-factor is determined as the ratio between soil temperature and air temperature (T_s/T_a). This is conceptually a factor summarizing the energy balance at the soil surface (Klene, et al., 2001b). Because this report focus on thawing of the active layer, the thawing n-factor also called nt-factor has been applied.

Vegetation influences the nt-factor - higher nt-factors are associated with sparse vegetation and lower nt-factors are associated with more vegetated areas.

Such a relation is found by Westermann et al. (2014) where vegetation is represented by a Normalized

Difference Vegetation Index (NDVI). Deriving an nt-factor based on NDVI values can be useful as air and surface temperature data can be limited (Klene, et al., 2001a). Interpolating air and surface temperatures from widely distributed climate stations (as is often the case in Arctic) is problematic as both air temperature and surface temperature varies spatially. Air temperatures vary both horizontal along latitudinal gradient and with a coast/inland gradient as well as vertical along an altitudinal gradient (Rouse, 1991) (Fausto, et al., 2009). Surface temperature varies greatly on local scale depending on e.g. vegetation cover, precipitation and cloud cover (Bonan, 2008) (Street & Melnikov, 1990). By establishing a relation between the nt-factor and NDVI, the nt-factor can be estimated without complete knowledge of air and surface temperature.

NDVI data can be obtained by using optical sensors in the electromagnetic spectrum. The utility of using optical sensors facilitate a non-destructive, near-real-time vegetation monitoring (Bueren, et al., 2015) (Lebourgeois, et al., 2008). Different types of optical sensors exist, and NDVI data can be collected both from satellite and by use of several ground based methods. Each method has a set of integrated strengths and uncertainties, and a comparison between different methods can give a valuable insight into these.

The aim of this article is to apply and evaluate three different ground based types of ground-spectral sensors, a Skye sensor, a NDVI camera, and a Decagon Sensor, in order to compare their features and application-accuracy for vegetation monitoring. The obtained NDVI values are used to estimate the nt-factor based on an established relation between NDVI and nt-factor for the study area. The nt-factors will be used in calculating the active layer thickness further described in the paper *'The Impact of Different Incorporated Factors in Active Layer Thickness Modelling using Stefan Solution'*.

2 Theory

The Normalized Difference Vegetation Index (NDVI) is an index of ‘greenness’ based on absorption and reflection of specific wavelengths. Green leaves absorb incoming solar radiation in the

visible spectrum in order to gain energy for photosynthesis (Pettorelli, 2013). Especially the red wavelengths (620-750 nm) are absorbed. As absorption of the incoming solar radiation in the near-infrared spectral region would cause the plant to overheat, near-infrared radiation (750-1400 nm) is reflected (Pettorelli, 2013). NDVI can be calculated simply as a ratio of the difference between the red and near-infrared reflectance over their sum (Pettorelli, 2013):

$$NDVI = \frac{(NIR - R)}{(NIR + R)} \quad (Eq. 1)$$

NDVI can thus be used as a measure for the amount of green, healthy vegetation (photosynthetically active material) within a specific spatial unit.

The index vary between + 1.0 and - 1.0. The higher reflectance of near-infrared wavelengths results in positive values for vegetated areas. Non-photosynthetic elements reflect both visible and near-infrared radiation and thereby show a small difference between the two bands (low NDVI). Negative values correspond to absence of vegetation or surfaces such as open water, snow or ice (Holben, 1986). According to Myneni et al. (1997) deserts, inland water bodies, and exposed soils have NDVI values ranging between -0.2 and 0.05. The NDVI for a given area will vary with life cycle of the vegetation within the area and thus season and depend on the availability of nutrient and water to support vegetation growth. Senescent vegetation has less chlorophyll and hence less absorption of red light and less reflection of near-infrared light, leading to reduced values of NDVI (Pettorelli, 2013).

NDVI values can be obtained from satellite images or via different ground-based methods. In-situ methods are often used to correct or validate satellite-based measurements (Decagon Devices, Inc., 2015). Different factors may influence NDVI measurements, affecting the reliability or usefulness of NDVI as a tool for estimating vegetation indices (Pettorelli, 2013). Values are seen to have a higher uncertainty in non-homogenous areas, especially in

areas where vegetation is adjacent to non-vegetated patches. Changes in surface water regime, either by precipitation or evapotranspiration, also influence the measurement of NDVI. Water on vegetation surface or ground surface absorbs more near-infrared light resulting in lower NDVI. This means that changes in NDVI could be due to altered soil moisture content and not changes in vegetation (Pettorelli, 2013). Since NDVI is calculated by the means of incoming solar radiation, atmospheric conditions such as presence of clouds, water vapor, or atmospheric contaminants likewise influence the NDVI values, often negatively leading to lower NDVI values (Pettorelli, 2013). Topography and altitude also affect NDVI measurements which makes comparing NDVI values for topographically variable areas problematic (Pettorelli, 2013).

Based on NDVI values as proxies for vegetation, Westermann et al. (2014) found a strong empirical correlation between NDVI and the nt-factor from Zackenberg, Kobbefjord and northern Alaska, computed for NDVI values from grid cell of 10*10 m and temperature data from a fixed installation, averaged over 7-10 days. Figure 1 shows the established relationship between NDVI and nt. Equation 2 shows the correlation represented by the black trendline.

$$n_t = 2.42 \cdot NDVI^2 - 3.01 \cdot NDVI + 1.54 \quad (Eq. 2)$$

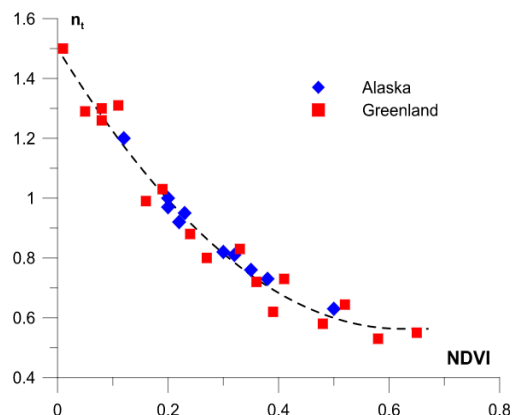


Figure 1. The relationship between NDVI and nt with data from Zackenberg, Kobbefjord (Greenland) and from Kuparuk River basin (northern Alaska). From Westermann et. al. (2014).

3 Methods

Later modelling of the active layer thickness (see paper: *The Impact of Different Incorporated Factors in Active Layer Thickness Modelling using Stefan Solution*) is based on investigating three transects with different vegetation (transect A, B and C). For this reason, these transects will be the focal point of this investigation and NDVI and nt-factors are estimated for each transect. Each transect contains 10 plots extending from south to north and are further described in Chapter 2.5 Site description.

Ideally, the three methods of measuring NDVI would result in more or less the same NDVI value for each plot and show a strong correlation when compared. The approach for investigating the three different methods is therefore based on establishing relationships between the methods in order to detect divergent behavior and thereby the reliability of the applied method. The three methods are a Skye 2 Channel Sensor (SKR 1800), a Decagon Spectral Reflectance Sensor (SRS), and a Canon SX260hs NDVI camera. The data were collected as an ongoing process over various environmental sites to compare the sensors in terms of their ability to produce reliable reflectance data. All sensors (Decagon, Skye and camera) shared a spectral range in the visible and near-infrared spectrum (VNIR, 400-1400 nm) which is considered the most relevant region of the electromagnetic spectrum for vegetation application (Bueren, et al., 2015). NDVI values are collected for each plot in the three transects, using the hand held Skye Sensor and the NDVI camera. Furthermore, NDVI values for an additional 35 plots randomly distributed across Blæsedalen are collected by use of both NDVI camera, Skye Sensor, and the Decagon sensor. The Decagon sensor was brought in based on a suspicion that the Skye Sensor did not provide reliable results. Because NDVI measured by Decagon sensor was not applied on the three transects, the correlations between the three investigated methods are examined for the 35 additional points where NDVI is measured by the use of all three methods.

The Skye sensor is a two channeled Spectral Reflectance Sensor facing only downwards. It measures reflected light in the red and infra-red spectrum and returns absolute values of NDVI. The device has a 25 degrees cone field of view, thus making the area measured a function of the height above the ground (Skye Instruments Ltd., 2015). The Skye sensor was held at a height approximately 0.6 m above the ground.

For Spectral Reflectance Sensors, a pair of identical sensors is usually used to measure incident and reflected light simultaneously, to eliminate variations in natural solar radiation during measurement. However, the Skye sensor in use did not take incoming light from the hemisphere directly above the sensor into account, since only a downward facing sensor was included. Absence of incident radiation affects the NDVI but can be accounted for by rearranging the vegetation index equation (Equation 3):

$$\begin{aligned} NDVI &= \frac{R_n/I_n - R_r/I_r}{R_n/I_n + R_r/I_r} = \frac{(I_r/I_n)R_n - R_r}{(I_r/I_n)R_n + R_r} \\ &= \frac{\propto R_n - R_r}{\propto R_n + R_r} \quad (Eq. 3) \end{aligned}$$

R_n is the reflected NIR radiation and R_r is the reflected red radiation, while I_n and I_r is the incident NIR and the incident red, respectively. With this rearrangement it is possible to determine the NDVI without direct values for the incident radiation – thus, it is required that the ration between the RED and NIR spectral irradiance (the alpha-value (I_r/I_n)) is known (Decagon Devices, Inc., 2015)

Alpha values for the time of the measurements on the 35 additional plots are obtained from a fixed climate station located at Østerlien. Alpha values are ranging from 1.23-1.29 with an average of 1.26.

The Decagon sensor is likewise a Spectral Reflectance Sensor for measuring NDVI of plant canopies. The sensor is a two-band radiometer, measuring incident radiation from above and reflected radiation from the surface. Incident radiation from the hemisphere is measured with a NDVI-hemispherical spectrometer with a viewing angle of 180 degrees while the reflected canopy radiation is measured with a NDVI-field stop

spectrometer that has a limited viewing angle of 36 degrees (Decagon Devices, Inc., 2015).

The applied NDVI camera is an original RGB digital camera (measuring radiation in the Red, Green and Blue spectral bands), modified to include radiation in the near-infrared (NIR) band. This modification removes the original near-infrared-blocking filter in the camera and replaces it with another band-pass filter – in our case a red-light-blocking filter (Bueren, et al., 2015) (Lebourgeois, et al., 2008). We used a special designed vegetation-sensing filter to include near infrared band and exclude the red light. With this approach we were able to calculate the blue NDVI vegetation index with the incoming NIR, Green and Blue light (NGB). The concept of measured radiation from an original RGB camera and the transformed camera is presented in Figure 2.

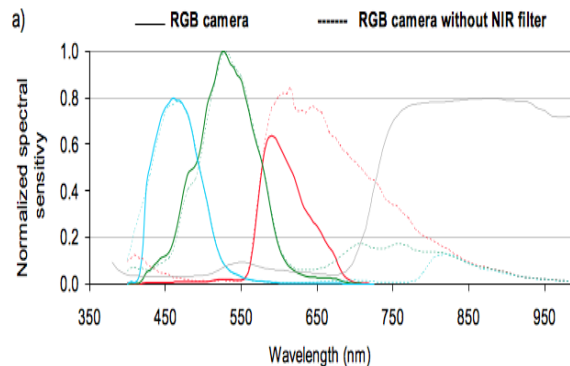


Figure 2. Concepts of the RGB (solid lines) and NIR-transformed camera. The RGB camera without NIR filter measures radiation in the NIR band instead of the red band. The grey line is a standard reflectance profile of a green vegetation canopy. The colours of the lines represent the camera channels. From Lebourgeois et al., 2008.

Using the blue band instead of the red band when calculating the vegetation index produces relative NDVI values and not absolute NDVI values of the covered areas (Lebourgeois, et al., 2008). Thus, pictures from the NDVI camera need to be processed in order to get actual NDVI values. In order to transform the images into NDVI-values, reference plates and Fiji imageJ software were initially applied. However, this approach showed no sufficiently accurate results. Instead, each picture was cropped into an area corresponding to the covered area by the Skye and Decagon sensor (for the 35 additional points). Both sensors are held at a

height 0.60 m above the ground, corresponding to an area of approximately 0.25*0.25 m (Skye Instruments Ltd., 2015) (Decagon Devices, Inc., 2015). By the means of MATLAB, relative NDVI values are calculated by use of the near-infrared and blue band. Because the MATLAB approach with camera NDVI does not provide absolute NDVI values, direct comparison of NDVI values with those obtained from Skye sensor and Decagon sensor is not possible. In order to obtain absolute NDVI values from the camera for the three transects, the relative values are converted to absolute NDVI values based on the found relation between NDVI from the camera and NDVI from the Decagon sensor.

Pre-setting of camera features such as exposure time, shutter release interval, and image format and size is possible due to the camera firmware (Bueren et al. 2015). Our converted near-infrared camera was set to both fixed (TV) and automatic Exposure Time (P) (fixed value of 1/1000 sec., automatic values between 1/250-1/1000 sec.). However, as Figure 3 illustrates, the resulting relative NDVI values plotted against each other show no marked distinction from the 1:1-line. In later processing of data, images with automatic Exposure Time have been used. With automatic Exposure Time, the camera adjusts for different lighting conditions and thereby indirectly adjust for different solar radiation. It can therefore be argued that alpha-correction of NDVI-values are unnecessary.

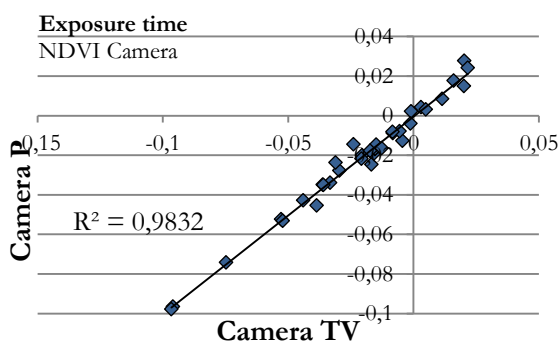


Figure 3. Fixed (TV) and automatic (P) exposure time. Based on data from the 35 additional plots

A relationship between NDVI and nt-factor is established by use of available temperature data from fixed and mobile climate stations. The mobile climate station has been located at areas adjacent to transects A, B and C for a total of seven days¹, measuring surface temperature (T_s), air temperature (T_a) and NDVI. Surface temperatures measured by the mobile climate station are taken above the ground and are actually measuring temperatures on the vegetation surface and not soil surface. In order to overcome this possible difference in temperature, measured surface temperatures from the mobile climate station are corrected. A correction factor is calculated from soil and vegetation surface temperatures from the fixed station at Østerlien as it was the only climate station measuring both temperatures (correction factor = $T_{\text{soil surface}}/T_{\text{vegetation surface}}$). The correction factor is assumed to be the same for all the sites.

In order to include as much data as available for a more reliable establishment of the nt-NDVI relationship, two fixed stations are included, one located at the CALM site and one near the coast. Only temperatures are measured so NDVI values are obtained from Landsat 8 (for the CALM site) and estimated to be zero (at the coast location) based on a lack of vegetation (Pettorelli, 2013).

The relation between NDVI and nt-factor for the total of nine data points is presented in Figure 4. A good correlation ($R^2 = 0.7803$) between NDVI and the nt-factor for the nine data points is found. This correlation is used to estimate values for nt-factor for the three transects based on NDVI (see chapter 4. Results).

¹ The mobile climate stations was put up for 9 days but failed to log NDVI values for two of the days at transect B. Thus, data are obtained for two days adjacent to transect A, one day adjacent to transect B and four days adjacent to transect C.

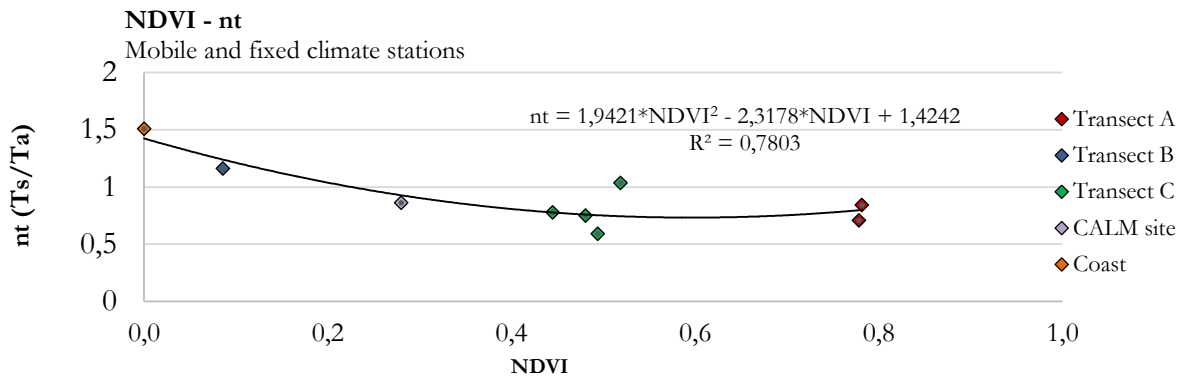


Figure 4. NDVI and nt-factor for nine data points distributed over five different locations. Each point resembles one day. Note that the mobile climate station was not located exactly at Transect A, B, and C but in areas corresponding to those of the transects.

4 Results

Relative and absolute values of NDVI from Skye, Decagon and camera is compared. When establishing a relation between absolute NDVI values from the Decagon sensor and relative NDVI values from the camera, a correlation of $R^2 = 0.6766$ is found (Figure 5).

Correlations between NDVI values from the Skye sensor and Decagon sensor (a) are presented in Figure 6 together with comparison between Skye sensor and the relative values from NDVI camera (b). A poor correlation between values are observed with $R^2 = 0.2996$ (a) and $R^2 = 0.1137$ (b), respectively.

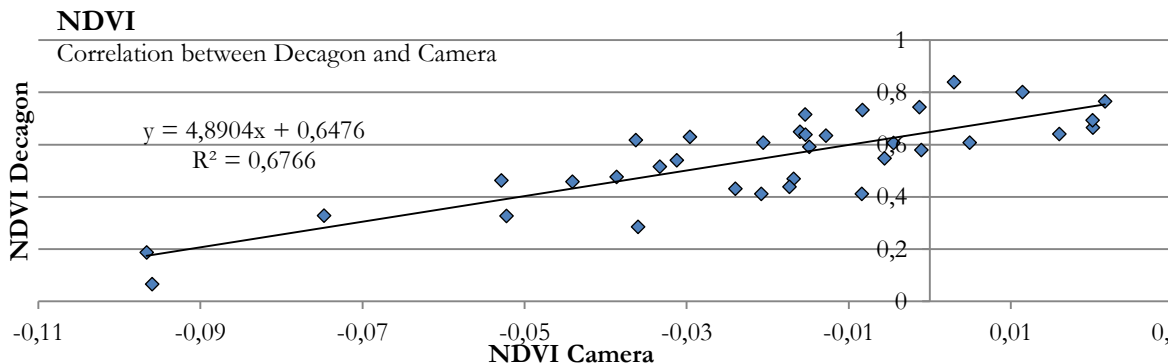


Figure 5. Correlation between absolute NDVI value from the Decagon sensor and relative values from NDVI camera.

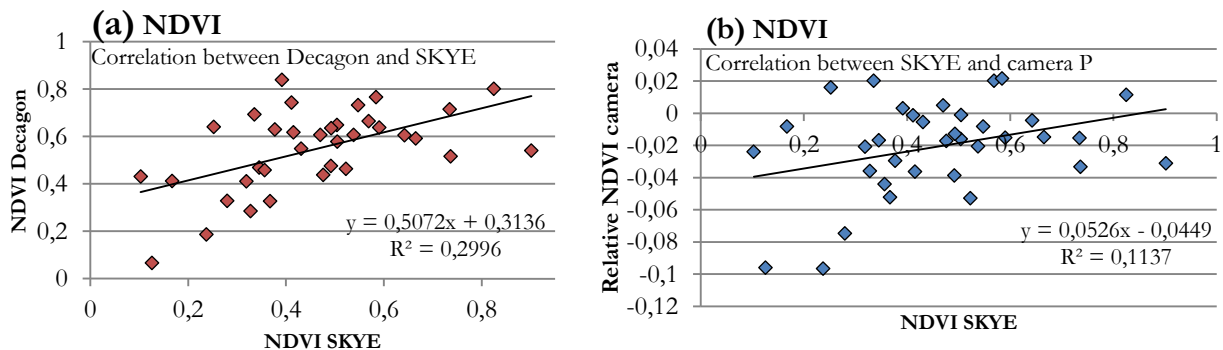


Figure 6. Figure (a) shows the correlation between absolute NDVI values from the Decagon sensor and the Skye sensor. The correlation between absolute NDVI values from the Skye sensor and relative NDVI values from the camera is shown in Figure (b).

The above mentioned results reveal how only values from camera and Decagon sensor show an acceptable correlation. This indicates that the Skye sensor is not measuring NDVI values corresponding to values obtained by the Decagon sensor and the NDVI camera.

In order to estimate the active layer thickness (see paper: *'The Impact of Different Incorporated Factors in Active Layer Thickness Modelling using Stefan Solution'*) the NDVI value for the three transects has to be found. Since no Decagon NDVI values exist for the three transects and the camera NDVI values for transects are relative values, the relation between camera and Decagon is used to adjust the relative camera values to absolute NDVI values. Thus, all camera values are transformed into absolute NDVI values via Equation 4.

$$NDVI_{adjusted} = 4.8904 \cdot Camera\ NDVI + 0.6476 \quad (Eq.\ 4)$$

Resulting absolute values for NDVI for the three transects are presented in Figure 7.

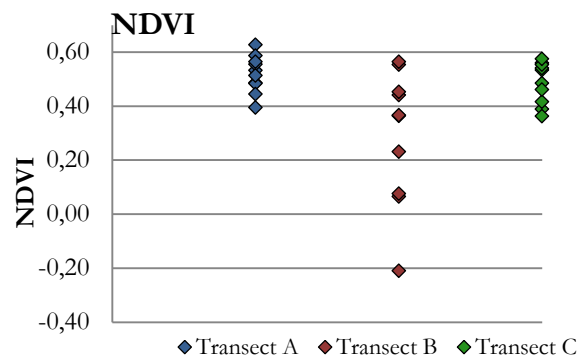


Figure 7. Absolute values for NDVI based on decagon-adjusted camera values; transect A (blue), B (red) and C (green).

The estimated average NDVI are 0.52, 0.29, and 0.49 for transect A, B, and C, respectively. Transect B has a significant lower average NDVI value than transect A and C. This lower NDVI is primarily caused by the dominance of bare soil in the first three plots of the transect. The figure also shows the occurrence of a negative value of NDVI for Plot 2 in transect B which will be discussed later.

From NDVI values, the nt-factor for the three transects can be estimated. This is accomplished by using the established relationship between NDVI and nt-factor based on mobile and fixed climate stations, described previously. The nt-factors for the different NDVI values are presented in Figure 8. For comparison, nt-factors calculated based on the relationship established by Westermann et al. (2014) is also shown in the figure.

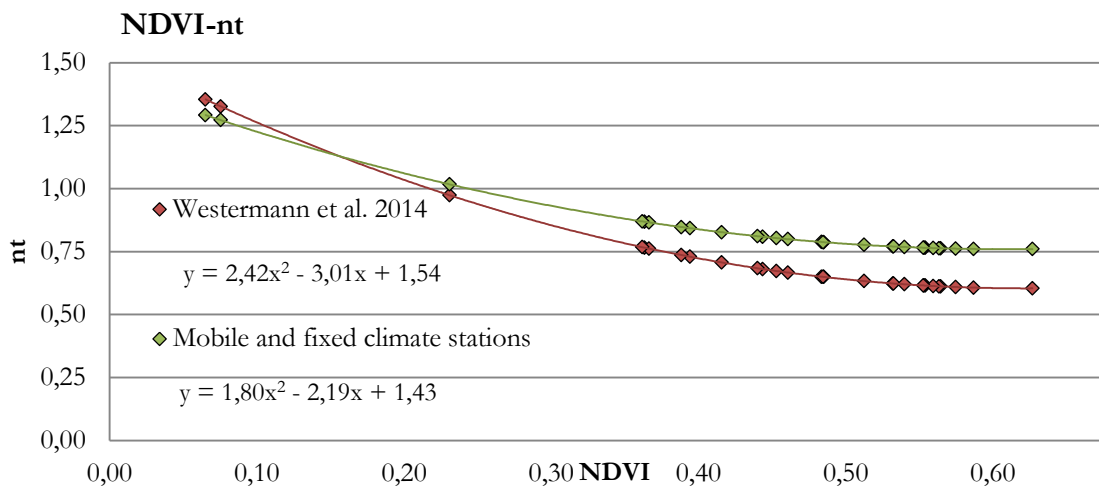


Figure 8. Estimated nt-factors for different transect NDVI values. Green points mark nt-factors calculated based on relationship between NDVI and nt-factors for climate stations in and around Blæsedalen whereas red points are nt-factors calculated based on the relation established by Westermann et al., 2014.

Figure 8 illustrates how the established relationship from climate stations has higher nt-factors than the relationship from Westermann et al. (2014) for NDVI higher than 0.15. Furthermore, nt decreases with increasing NDVI value. Figure 9 present the nt-factors for each transect, calculated from the established relation from climate stations.

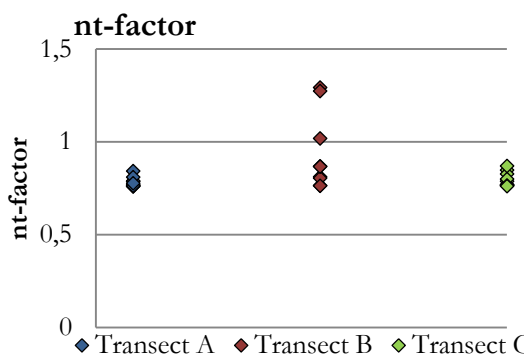


Figure 9. nt-factors for transect A, B and C, calculated based on the established relation from climate stations.

Nt-factors ranges from 0.76 to 1.27 with Transect B having the highest mean nt-factor of 0.90 and Transect A and C having a lower mean nt-factors of 0.78 and 0.80, respectively.

5 Discussion

Ideally, the three different methods should show more or less the same relative pattern for the 35 additional points. However, the Skye sensor showed no consistency with the Decagon sensor or camera and the best correlations was found to be $R^2 = 0.6766$ between Decagon sensor and the camera. Several factors can contribute to these observed patterns.

As mentioned previously, the measurement of NDVI can especially be influenced by atmospheric and meteorological conditions. Such influences could lead to incorrect NDVI values. In order to investigate whether noise in the relations is related to these influences, NDVI values have been investigated for dependency to incoming solar radiation (S_i) as a proxy for the atmospheric conditions. Furthermore, influence of precipitation is considered.

In Figure 10, the influence of S_i on measured NDVI is presented based on data from the mobile climate station in the period 06.08.2015 to 08.08.2015 when the station was located in Blæsedalen.

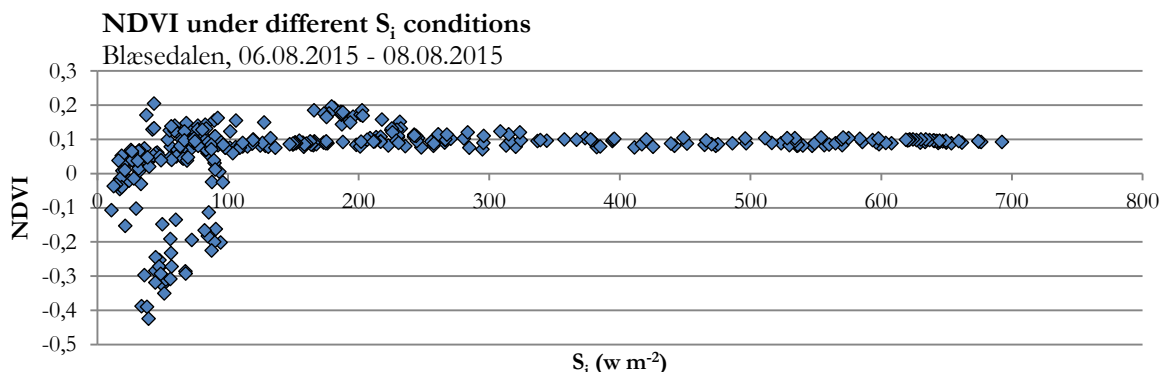


Figure 10. NDVI under different S_i conditions. NDVI proved to be constant under changing S_i conditions above 100 W m^{-2} . Values from a mobile climate station located in Blæsedalen, 06.08.2015-08.08.2015.

Figure 10 shows how NDVI values are more or less constant with S_i values exceeding 100 W m^{-2} . S_i lower than 100 W m^{-2} resulted in fluctuating NDVI measurements, which should not occur as the location was fixed and the measurements conducted within a short time span. Because of this, NDVI measured at S_i below 100 W m^{-2} is not considered reliable. This relation between S_i and NDVI does not include the Skye sensor as explained in the following section.

For the three transects, S_i was found to be between $175\text{-}910 \text{ W m}^{-2}$ in the period where NDVI by Skye sensor and the camera was measured. For NDVI measured by the Skye sensor, the following relation with corresponding S_i values has been observed (Figure 11).

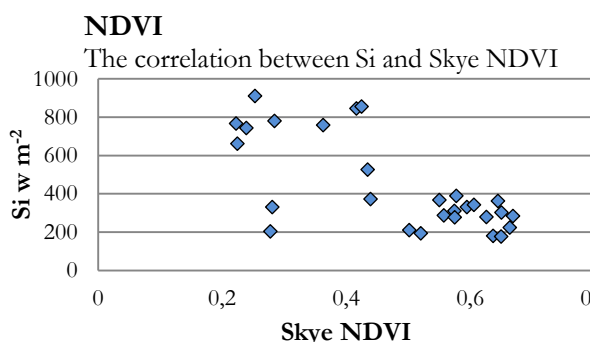


Figure 11. The relation between NDVI measured by Skye sensor and incoming solar radiation (S_i) for the transect plots. The first two plots of Transect B have been excluded from the graph due to their low vegetation cover and corresponding low NDVI value.

In Figure 11, two clusters can be detected. One cluster has high NDVI values, above 0.5, and S_i

values below 400 W m^{-2} , where the second cluster has NDVI values lower than 0.5 but higher S_i values (besides from three points). A significant difference in NDVI between the two clusters exists, indicating that NDVI is dependent on incoming solar radiation (for the Skye sensor) as measured NDVI is lower for high S_i values, and higher for low S_i values. This dependency is problematic for the Skye sensor method as the NDVI values are alpha-corrected and incoming solar radiation should be accounted for. Because of this dependency with S_i , despite the alpha-correction and because of the poor correlation with NDVI values from the camera and Decagon sensor, NDVI obtained from Skye sensor are not considered reliable and application can lead to misguided conclusions.

This conclusion is supported by Decagon Devices, Inc. (2015) which states that alpha-values are affected by changing atmospheric conditions and the solar elevation angle and direct measurements of incident radiation give more accurate results of NDVI.

When correlating S_i with camera NDVI values upscaled to absolute values by the relation between camera and Decagon sensor, no clear trend is seen. This suggests that measurements of NDVI by the camera and Decagon sensor are less dependent of incoming solar radiation and thus more reliable estimates of vegetation than NDVI derived from Skye sensor (see Figure 12).

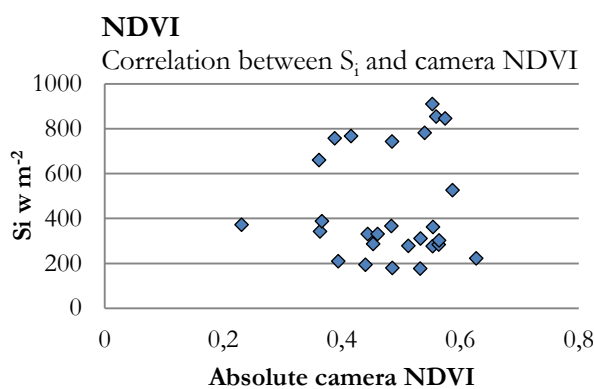


Figure 12. The relation between incoming solar radiation (S_i) and NDVI measured by the camera and upscaled to absolute values by the relation between camera and Decagon sensor for the additional plots. The first three plots of Transect B have been excluded from the graph due to their low vegetation cover and corresponding low NDVI value.

During the sampling period, several precipitation events occurred. A wet soil surface absorbs near-infrared wavelengths which lowers the NDVI. Measuring NDVI right after a rain event could lead to false NDVI values.

For instance, the correlation between Decagon and camera values has a zero point ($\text{NDVI}_{\text{adjusted}} = 0$) at camera values equal to -0.13. Thus, values below this will result in negative absolute NDVI values after adjustment, as is the case for plot 2 in Transect B which was estimated to have a NDVI of -0.21 (Figure 13).



Figure 13. The area under investigation (approx. 0.25×0.25). Transect B, plot 2:Abrasions plateau east of Blæsedalen.

Typically negative values of NDVI correspond to snow, ice, and water (Holben, 1986). As Figure 13 indicates, the area of plot 2 in Transect B is dominated by bare soil and stones, with black lichen

and a single fireweed (*Chamerion latifolium*) present as well. NDVI for bare soils typically range from 0.0-0.1 (Pettorelli, 2013) (Holben, 1986). Further Myeni et al. (1997) found that exposed soils have NDVI values ranging between -0.2 and 0.05.

If a rain event had happen before the measurements were taken, the soil surface could be saturated and wet, causing the NDVI to be negative. However, rain gauges located at Østerlien show no considerable precipitation in the days before measurements were taken.

Besides meteorological conditions, other sources of error can influence the results. The Skye sensor might give incoherent values due to methodological mistakes; if the sensor has not always been held completely horizontal or if any of us accidentally has been shading the area under study (as mentioned as an error source by Skye Instruments Ltd. (2015)). To overcome problems with shading both Skye sensor measurements and camera images have been taken facing the sun.

A likely source of uncertainty is related to the height above the ground at which the sensor was held, and the corresponding cropping of camera pictures. A height of 0.6 m has been assumed for all measurements. According to User Manuals for both Decagon and Skye sensor, this corresponds to a covered area of 0.05 m^2 , shaped as a circle with radius approximately 0.13 m (Decagon Devices, Inc., 2015) (Skye Instruments Ltd., 2015). However, for practical reasons the camera images are cropped as a square with length two times the radius (approximately 0.25 m). This results in a slightly enlarged area (0.06 m^2) where the included part in the corners could have different vegetation cover than the middle part and thus potentially influencing the final NDVI value for this plot as a whole. However, only small discrepancies are expected and photo material from the plots have been investigated to ensure that no marked difference in vegetation cover exist between a circle and square-area. Likewise, different people holding the sensor together with different posture might influence the actual area under investigation. A higher elevation of the sensor at e.g. 0.75 m will

result in a covered area of 0.34×0.34 m (0.09 m 2). Thus, sensor values would be compared with camera values from a smaller area.

To gain comparable NDVI values between the three methods, the exact same area had to be investigated. Where the vegetation is very patchy and scattered this could lead to different NDVI values if the three methods are not measuring the same 0.05 m 2 .

Average NDVI values for the three transects were estimated to be 0.52, 0.29, and 0.49 for transect A, B, and C, respectively. This ranking of average NDVI between the three transects is somewhat expected.

Transect B had a larger soil cover fraction which is expected to cause the lower NDVI. Transect A and C have similar average NDVI values, although they vegetation wise were very different. Transect A was dominated by plants like Vaccinium and Salix, whereas Transect C was dominated by water tolerant plans like mosses and horsetail. Further validation of our estimated NDVI values for the

three transects is brought by a comparison with NDVI derived from satellite images. NDVI derived from satellite data from 28.07.2015 for the three transects are presented in Figure 14.

Satellite NDVI values range from 0.39-0.49 for Transect A, 0.29-0.30 for Transect B, and 0.31-0.43 for Transect C. Opposite of the in situ methods, Landsat estimates almost no variability between plots at transect B. The NDVI values derived from Landsat 8, are in general lower compared to the in situ methods. This could be due to influence of the scale differences, where Landsat measure NDVI on a larger area of 30×30 m. The NDVI from Landsat shows the same tendency with lowest values at Transect B and highest at Transect A, and are easily comparable. Satellite NDVI can provide an overview of the general greenness of a larger area but does not provide the same accurate vegetation index as the Decagon sensor or the camera. The measurement made at transects have showed how much NDVI variates within even small distances, and are therefore more trustworthy in small-scale fieldwork.

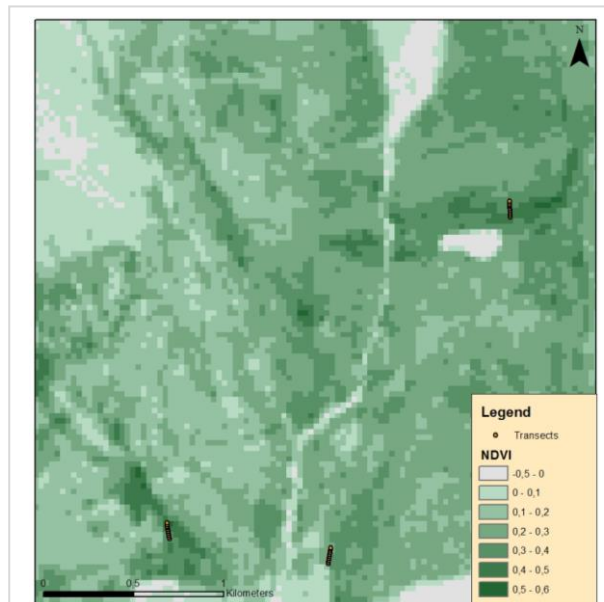
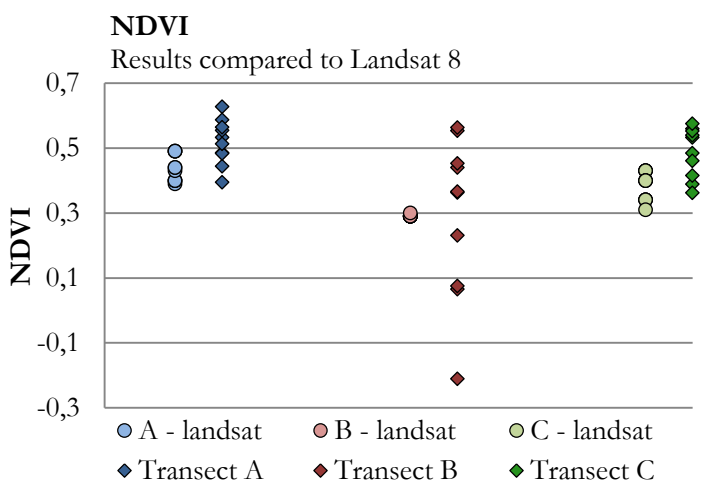


Figure 14. NDVI from Landsat 8 (28.07.2015) for the transects A (most left), B (lower right) and C (upper right corner of picture).



The relation between NDVI and nt-factor shows how nt decreases with increasing NDVI values. This is expected as vegetation canopy lowers the surface temperature by reducing the amount of solar radiation reaching the ground and evapotranspiration cools the surface (Street & Melnikov, 1990) (Bonan, 2008). Where there is no vegetation to act as a buffer between the surface and air, the difference between these two temperatures becomes less or even higher surface temperatures than air temperatures can occur, leading to greater values for nt. That is the case for Transect B. Opposite where there is plenty of vegetation, surface temperatures are lower than the air temperatures leading to lower values of nt.

As presented in Figure 8, the nt-NDVI correlation for the three transects based on climate stations in Blæsedalen and Østerlien has calculated higher nt-factor values than those based on the relation established by Westermann et al. (2014).

One of the main reasons for this difference is thought to be related to differences in climate data sampling. The data used by Westermann et al., 2014 is average surface and air temperatures measured over 7-10 days from fixed climate stations in Zackenberg and in Kobbefjord. Furthermore, values of nt and NDVI from the Kuparuk River basin in northern Alaska, derived from Klene et al. (2001a) and Walker et al. (2003), are included (Westermann, et al., 2014). In the present investigation, data origins from a much shorter period as the mobile climate station was only measuring an area for 1-4 days before moving to another location. As surface temperature varies greatly due to e.g. wind, precipitation, and cloud cover, a shorter time span of measuring these climate data could cause the difference in nt-factors between our results and those derived from Westermann et al. (2014). Furthermore, the NDVI values in this investigation are obtained between 10 am to 15 pm in order to avoid bias from atmospheric conditions. As the data from Westermann et al. (2014) are averaged they also include measurements taken outside the time span used in this investigation. This would quite possibly result in lower temperature values for both surface

and air as well as lower the NDVI values causing the relationship established by Westermann et al. (2014) to be lower than the relationship based on climate stations.

Additionally, our relationship between nt-factor and NDVI is based on several assumptions. As mentioned two fixed climate stations (CALM-site and Coast) have been included in establishing the relationship in order to include more data and thereby a more reliable estimate. The CALM-site point is based on NDVI values from Landsat 8 as in situ data was not available. The resolution of 30*30 might result in different NDVI than the actual value corresponding to surface temperature measured below the sensor.

With respect to NDVI values for Coast, NDVI was assumed to be zero due to lack of vegetation which generally results in NDVI values close to zero (Pettorelli, 2013). However, as shown in Figure 7, bare soil can also create negative NDVI values. These two assumptions are critical for the reliability of the relationship between nt-factor and NDVI. However, it is assessed that including data using these assumptions leads to less uncertainties than not including the two additional data points, CALM-site and Coast, in the establishment of the relation between nt and NDVI.

Other assumptions have been made regarding interpolation of climatic factors. The mobile climate station associated with transect C was not placed directly in the area of transect C, but near Østerlien in an area with corresponding wetness and vegetation type. It was assumed that the nt-factor obtained there would equal a nt-factor obtained at Transect C. However, as air temperature varies along both a coast/inland gradient and an altitudinal gradient, this assumption could as well alter the established relationship between nt and NDVI. Furthermore, when estimating the nt-factor from the mobile climate station, a correction factor have been used to account for the fact that the mobile climate station does not measure soil surface temperature, but rather vegetation surface temperature. This correction factor is based on the ratio between soil temperature and vegetation surface temperature for the fixed climate station at Østerlien and was assumed to be the same for the

four other sites. Again as temperature varies greatly over even small distances especially depending on topography, soil moisture, and vegetation cover, this assumption could likewise be problematic.

6 Conclusion

Evaluated measurements between NDVI and incoming solar radiation show a strong correlation – with a bias when solar radiation is below 100 W m^{-2} . The Skye sensor showed no consistency with the Decagon sensor or NDVI camera and is therefore dismissed. The Decagon sensor and NDVI camera showed more consistent values of NDVI. Thus, relative values from camera are converted to absolute NDVI values based on the established relation between NDVI from camera and Decagon sensor. Average NDVI are found to be 0.52, 0.29, and 0.49 for transect A, B, and C, respectively. NDVI obtained from Landsat 8 is generally lower than those obtained from in situ methods. This might be due to the large difference between spatial resolutions with Landsat measuring grids at $30 \times 30 \text{ m}$ while in situ methods focus on single plots of 0.25-0.25 m.

A relation between NDVI and nt-factor has been established after Westermann et al. (2014) by use of fixed and mobile climate stations in and around Blæsedalen. Surface temperature has been adjusted to account for the fact that the sensor is actually measuring vegetation surface temperature instead of soil surface temperature. From this relation and obtained NDVI, nt-factors for each plot have been calculated and will be used further in active layer thickness modelling (see paper: ‘*The Impact of Different Incorporated Factors in Active Layer Thickness Modelling using Stefan Solution’*).

Nt-factors ranges from 0.76 to 1.27 with transect B having the highest mean nt-factor of 0.90 and transect A and C having a lower mean nt-factors of 0.78 and 0.80, respectively. Nt-factors above 1 indicate higher surface than air temperatures and only occurs at transect B.

7 Literature

Bonan, G., 2008. *Ecological Climatology - Concepts and Applications*. 2. ed. New York: Cambridge University Press.

Bueren, S. K. v. et al., 2015. Deploying four optical UAV-based sensors over grassland: challenges and limitations. *Biogeosciences*, Issue 12, pp. 163-175.

Decagon Devices, Inc., 2015. *SRS Spectral Reflectance Sensor*, Pullman: Decagon Devices, Inc..

Fausto, R. S. et al., 2009. A new present-day temperature parameterization for Greenland. *Journal of Glaciology*, 55(189), pp. 95-105.

Holben, B. N., 1986. Characteristics of maximum-value composite images from temporal AVHRR data. *International Journal of Remote Sensing*, 7(11), pp. 1417-1434.

Klene, A. E., Nelson, F. E., Shiklomanov, N. I. & Hinkel, K. M., 2001a. The N-factor in Natural Landscapes: Variability of Air and Soil-Surface Temperatures, Kuparuk River Basin, Alaska, U.S.A.. *Arctic, Antarctic, and Alpine Research*, 33(2), pp. 140-148.

Klene, A., Nelson, F. & Shiklomanov, N., 2001b. The n-factor as a Tool in Geocryological Mapping. *Physical Geography*, 22(6), pp. 449-466.

Lebourgeois, V. et al., 2008. Can Commercial Digital Cameras Be Used as Multispectral Sensors? A Crop Monitoring Test. *Sensors*, Issue 8, pp. 7300-7322.

Myneni, R. et al., 1997. Increased plant growth in the northern high latitudes from 1981-1991. *Nature*, Volume 386, pp. 698-702.

Pettorelli, N., 2013. NDVI from A to Z. In: N. Pettorelli, ed. *The Normalized Difference Vegetation Index*. Oxford: Oxford University Press, pp. 30-43.

Riseborough, D. et al., 2008. Recent Advances in Permafrost Modelling. *Permafrost and Periglacial Processes*, Issue 19, pp. 137-156.

Rouse, W. R., 1991. Impacts of Hudson Bay on the Terrestrial Climate of the Hudson Bay Lowlands. *Arctic and Alpine Research*, 23(1), pp. 24-30.

Skye Instruments Ltd., 2015. *Skye: 2-Channel Light Sensor*, Llandrindod Wells: Skye Instruments Ltd..

Street, R. B. & Melnikov, P. I., 1990. Seasonal snow cover, ice and permafrost. In: W. M. Tegart, G. Sheldon & D. Griffiths, eds. *Climate Change: The IPCC Impacts Assessment*. Canberra: IPCC, pp. 257-293.

Walker, D. et al., 2003. Vegetation-soil-thaw-depth relationships along a low-arctic bioclimate gradient, Alaska: synthesis of information from the ATLAS studies. *Permafrost Periglac. Proc.*, Issue 14, pp. 103-123.

Westermann, S. et al., 2014. Future permafrost conditions along environmental gradients in Zackenberg, Greenland. *The Cryosphere*, Issue 9, pp. 719-735.

Westermann, S. et al., 2009. The annual surface energy budget of a high-arctic permafrost site on Svalbard, Norway. *The Cryosphere*, Issue 3, pp. 245-263.

Zhang, T., Osterkamp, T. & Stamen, K., 1997. Effects of Climate on the Active Layer and Permafrost on the North Slope of Alaska, U.S.A.. *Permafrost and Periglacial Processes*, Issue 8, pp. 45-67.

The Impact of Different Incorporated Factors in Active Layer Thickness Modelling using Stefan Solution

Maja la Cour Bohr¹, Peter Bo Mähl¹, Stinna Susgaard Filsø¹, Søren Pierre Aagaard¹

¹Cand.Scient Stud, Geography and Geoinformatics, Department of Geosciences and Natural Resource Management, University of Copenhagen

Abstract

Active layer thickness for three transects on Disko Island is calculated and the impact of different controlling factors of the active layer thickness is investigated. Stefan Solution is applied and soil properties for calculation of an edaphic factor is derived from soil samples (bulk density, water content, soil organic matter, and texture) and in situ measurements of thermal conductivity. The input climatic factors are Potential Radiation Index, Degree Days of Thaw and nt-factor, the latter estimated from NDVI by use of an established empirical relation from in and around Bæsedalen. Active layer thicknesses is calculated to be 0.74, 0.77, and 0.81 m (average values) for transect A, B, and C. No marked difference in active layer thicknesses are observed between transects despite differences in wetness and vegetation cover. Calculation of active layer thickness proved to be highly sensitive to thermal conductivity, highlighting the importance of reliable instruments. Comparison of DDT from different fixed climate station emphasize the importance of using temperature data from the area under investigation, as temperature vary greatly even on smaller distances due to elevation- and coastal gradients.

Key words: Edaphic factor, active layer, permafrost thawing, PRI, DDT.

1. Introduction

Active layer thickness is a great indicator of how climate changes influences the Arctic region. The depth of the active layer (Z) can be estimated based on a modified Stefan solution derived from Zhang et al (2005):

$$Z = E \cdot \sqrt{n_t \cdot PRI \cdot DDT} \quad (Eq. 1)$$

In this equation, E is a measure of the edaphic factor, PRI is the potential radiation index, DDT is degree-days of thaw and n_t equals the n-factor of thaw ($= T_s/T_a$). The modified Stefan equation is composed of an edaphic term (E) and a climatic term (n_t , PRI, DDT) (Nelson & Outcalt, 1987).

The edaphic factor (E) is a term considering what influence soil thermal properties have on the active layer thickness. The thermal regime of the soil is primarily a constitution of the soil's ability to store and conduct heat (Bonan, 2008). This ability is especially controlled by the soil texture, porosity, organic matter content, and soil moisture. The edaphic factor, and thereby the influence of soil thermal

properties on active layer thickness, is calculated by the following equation (Nelson & Outcalt, 1987).

$$E = \sqrt{\frac{2K_t S}{P_b w L}} \quad (Eq. 2)$$

K_t is thermal conductivity ($\text{W m}^{-2} \text{ K}^{-2}$), S is a scale factor (s day^{-1}), P_b is bulk density of the soil (kg m^{-3}), w is water content (kg kg^{-1}), and L is latent heat of fusion (J kg^{-1}). Thermal conductivity is the ability of a material to conduct heat. Zhang et al. (2005) found this parameter to vary with bulk density, water content and type of the soil. Solids like quartz have a very high thermal conductivity, higher than clay and both air and water (Bonan, 2008). Soil porosity determines the fraction of solids, air, and water in the soil and is a function of organic matter and bulk density, which is a measure of how compact the soil is. Latent heat of fusion expresses the required amount of energy for a material to change phase from solid to liquid without change in temperature of the specific matter. Thus, the above stated equation represents a sum of abiotic factors and thereby an overall soil parameter.

The climate term represents proxies for exchanges of energy between surface and atmosphere and is here the nt-factor, Potential radiation index (PRI) and Degree Days of Thaw (DDT), respectively (Bonnnaventure & Lamoureux, 2013). The nt-factor relates ground surface temperature to air temperature and indicates if there is a buffer between soil and atmosphere that can alter or protect the ground thermal regime from the atmospheric thermal regime. In summer, this relation between air and surface temperatures reflects the vegetation cover (Klene, et al., 2001). DDT is a thawing index, calculated as the accumulated departure of mean daily air temperature above 0 °C (Riseborough, et al., 2008). The index represents both magnitude of thawing temperatures and duration of thawing season and thus the cumulative values of DDT for a given summer can tell how cold or warm it has been and for how long (Polar Science Center, 2010). PRI is included to take into account the influence of topography on the incoming solar radiation, and hence the temperature (Klene, et al., 2001).

The aim of this paper is to model active layer thickness at three locations in and around Blæsedalen and to determine the impact of the different incorporated factors in this modelling.

2. Methods

Field work took place between the 2nd -12th of August 2015. Three transects are investigated, each stretching 100 m and comprising 10 equally spaced plots. These transects, A, B, and C, are located in or around Blæsedalen on Disko Island, providing a total of 30 plots. For a further description of transects see chapter 2.5 *Site description*. Transect sampling is a common technique for collecting soil samples in a sloping terrain and the locations of transects are based on criteria about covering different properties such as vegetation and wetness (Pennock, et al., 2008). Active layer thicknesses are modelled for three locations at Disko Island. The modified Stefan Solution for estimating the thickness of the active layer has been applied due to its applicability and its ability to utilize typically available data. All transect had a south-facing slope, to minimize the difference in PRI between transects.

2.1 Soil properties of transects

Input to edaphic factor was gathered for each plot at each transect in the soil beneath the O-horizon.

The soil properties were measured by soil samples and thermal conductivity and soil temperature was measured via a KD-2 pro Thermal Properties Instrument. The KD-2 instrument sends a large heating current through a sensor and the change in temperature is measured (Decagon Devices, Inc., 2015).

Two soil samples were taken for each plot: a ring sample from where bulk density and water content were calculated and a second sample to obtain soil organic matter and texture.

The ring samples were dried at 110 °C for 24 hours. The bulk density and water content were determined with the following two equations:

$$\text{Bulk density } (\text{kg m}^{-3}) = \frac{\text{Dry soil weight (g)}}{\text{Volume of ring sample (cm}^3\text{)}} \cdot 1000 \quad (\text{Eq. 3})$$

$$\text{Water content } (\text{kg kg}^{-1}) = \frac{\text{Volumen of water pr. volume soil (m}^3\text{m}^{-3}\text{)}}{\text{Bulk density } (\text{kg m}^{-3})} \cdot 100 \quad (\text{Eq. 4})$$

Soil organic matter content was estimated by loss of ignition. First the soil had to be milled into a homogeneous sample. Then it was burned at 1350 °C by the ELTRA furnace which provided an estimate of the total carbon. If assuming all the carbon derived from organic material, and that the carbon constitutes 58 % of the organic matter, organic matter can be calculated by multiplying total carbon content with a conversion factor of 1.72 (Breuning-Madsen & Krogh, 2005) (Edwards, et al., 1999). Texture was found by Hydro 2000G which analyzes the particle distribution of the soil samples.

2.2 Vegetation

Several methods were used to characterize vegetation at the transects. A pinpoint method provided a quality measurement of the vegetation and a measure of the cover fraction. The vegetation index was measured as NDVI with a hand held Skye sensor and NDVI camera. For a description of these methods, see paper '*Estimating NDVI and nt-factor on Disko Island, Greenland, using different in situ methods*'. The Skye sensor did not provide reliable NDVI values and since the NDVI camera only produced relative NDVI values, a relation between NDVI values measured with NDVI and the Decagon sensor was established for 35 additional plots distributed across Blæsedalen and Østerlien. NDVI values were moreover derived from satellite images.

2.3 Nt-factor

The in situ surface temperature measurement proved to be improbable and the nt-factor could therefore not be established from a simple T_s/T_a calculation. Instead, an nt-NDVI relationship was established. Nine data points at five different locations were incorporated in creating a correlation between NDVI and nt, as presented in paper '*Estimating NDVI and nt-factor on Disko Island, Greenland, using different in situ methods*'. This correlation was comparable to another study by Westermann et al. 2014, however produces slightly higher values for nt.

2.4 Degree Days of Thaw

The fixed climate station in Østerlien measured air temperatures on a 30 minutes interval. From these climate data, an average daily air temperature was calculated. Summing the number of degrees above 0 °C for each day throughout a whole year, gave the number of degree days of thaw (DDT). The climate station had complete data from 2013 and 2014 and the average DDT did not vary more than 35 degree days between the two years. Thus, DDT from 2014 was used in the calculation of the active layer depths. DDT calculated from the climate station in Østerlien was assumed to represent the DDT at the locations of the three transects.

2.5 Potential Radiation Index and growing season

Nelson et al. (1997) presents the following equation for calculating Potential Radiation Index (PRI):

$$PRI = \frac{R_s}{R_h} \quad (Eq. 5)$$

Where R_s is the potential global radiation for a sloping surface and R_h is potential global radiation of a horizontal surface. Both R_s and R_h are determined for the individual latitude, gradient and orientation. The ArcGIS tool *Area Solar Radiation* calculates the R_s and R_h by the following equation (ESRI, 2012):

$$R_{s,h} = Dir_{tot} + Dif_{tot} \quad (Eq. 6)$$

Where Dir_{tot} is direct radiation from sun map sectors and Dif_{tot} is diffuse radiation of sky map sectors. The transmissivity of the atmosphere was set to 70 % for this study area, based on the assumption of generally clear weather around midday in the growing season. With information about growing season,

ArcGIS could calculate both the R_s and R_h from the digital elevation model of Disko. Raster calculator in ArcGIS helped to create a PRI map of Blæsedalen.

NDVI index from Østerlien

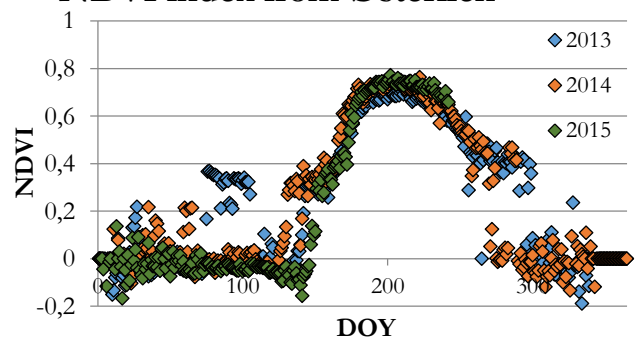


Figure 1. Daily NDVI measured at Østerlien climate station through the years 2013-2015.

The growing season was estimated from NDVI data derived from Østerlien climate station. Figure 1 shows daily NDVI measured at Østerlien climate station through the years 2013-2015.

In order to detect onset and offset of growing season, an approach similar to Karlsen et al. (2008) have been applied. Karlsen et al. (2008) provides a method for calculating the growing season with the help of NDVI measurement from MODIS data. To determine the onset of the growing season, the NDVI value had to exceed 85 % of the mean NDVI value for the summer period. The threshold for ending the growing season was set to 95 % of the mean NDVI value for the summer period (Karlsen, et al., 2008). To avoid a false onset or ending of the growing season, the NDVI was set to stay above or below the given threshold, respectively, for a coherent period.

In this case, the start threshold for NDVI was set to 0.4, which represent the value for the vegetation after snowmelt and before the growing season start. The end threshold was set to 0.5, which would be the lowest point where the vegetation stabilizes before the snowfall. Table 1 shows the growing season for year 2013 and 2014. The growing season used in the *Potential Radiation Index* calculation is the average of 2013 and 2014.

Table 1. Growing season

	2013	2014
Start of growing season	12-jun	12-jun
End of growing season	13-sep	21-sep
Growing season in days	93	101

3. Results

3.1 Edaphic factor

The edaphic factor is calculated by use of measured thermal conductivity, bulk density and water content as well as latent heat of fusion and a scaling factor.

3.1.1 Bulk density

Bulk densities are measured from ring samples and lies within the range 0.20 g cm^{-3} – 1.55 g cm^{-3} for the 30 plots. These values fit well with those from ring samples from Mariager & Nissen (2014), ranging from 0.16 – 1.40 g cm^{-3} . However, they evaluated their values to be too low, based on comparison with other methods. The obtained values might therefore be underestimated. In general though, low bulk densities can be related to high amounts of organic matter within the sample. According to the U.S. Texture classes, bulk densities of organic soils are around 0.3 g cm^{-3} (Campbell et al. 1994), which is lower than bulk densities of mineral soils. The organic content of the soil varies from 0.1 – 47% between the plots. An expected trend of decreasing bulk density with increasing organic matter content is observed in data. Further, soils with volcanic origin generally have lower bulk density (Breuning-Madsen, 2005) and the volcanic origin of Blæsedalen might therefore be the main reason for the low bulk densities. This suggests that our bulk densities are valid. In addition, Elberling et al. (2004) presented slightly higher values for bulk densities for some main soil types in Zackenberg, ranging from 0.6 - 1.8 g cm^{-3} .

3.1.2 Thermal conductivity

Thermal conductivities for each plot in the three transects are presented in Figure 2.

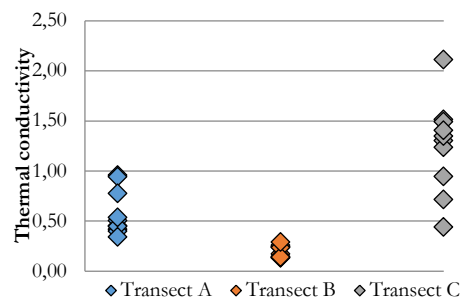
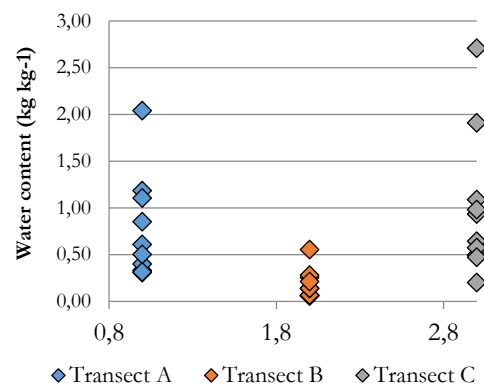


Figure 2. Thermal conductivities for 30 plots.

Highest thermal conductivities are found for transect C whereas Transect B has the lowest thermal conductivities. The values range from 0.13 - $2.11 \text{ W m}^{-1}\text{K}^{-1}$. Westermann et al. (2014) used a value of $3.0 \text{ W m}^{-1}\text{K}^{-1}$ for the mineral fraction of soil while Tritt (2004) stated that soil with organic matter has thermal conductivities between 0.15 - $2.0 \text{ W m}^{-1}\text{K}^{-1}$. The obtained values therefore fall within a realistic frame.

3.1.3 Water content

In the edaphic factor calculation, water content is given in the unit of kg kg^{-1} . The water content ranges between 0.06 - 2.71 kg kg^{-1} . Figure 3 presents water content for the 30 plots.

Figure 3. Water content (kg kg^{-1}) for the 30 plots.

3.1.4 Edaphic factor

The edaphic factor is calculated by use of the above mentioned values for thermal conductivity, bulk density, and water content and a value of 333660 J kg^{-1} for Latent heat of fusion (L). Furthermore, a scaling factor (S) of 86400 seconds day $^{-1}$ is incorporated. The resulting edaphic factors for each lot are presented in Figure 4.

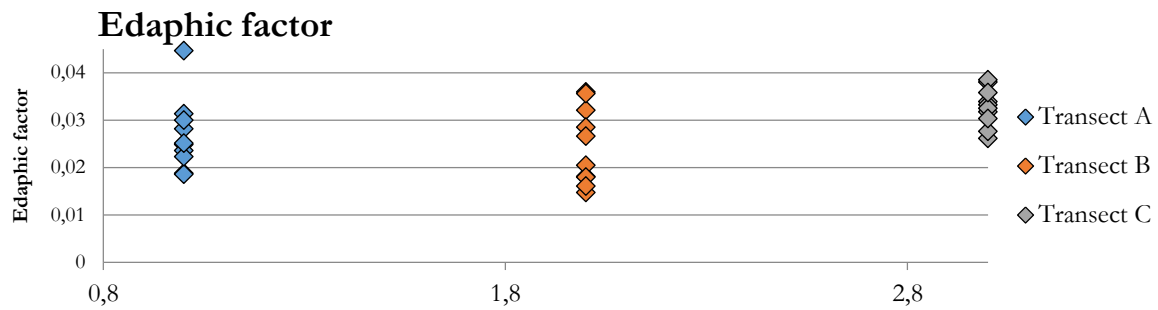


Figure 4. Edaphic factors for transect A, B and C.

The edaphic factors range between 0.015 – 0.045 for all plots, with an average of 0.028. Transect C seems to have slightly higher overall values of edaphic factor than Transect A. Transect B has a trend of decreasing edaphic factor with increasing plot number, corresponding to increasing vegetation cover, ranging from little to fully vegetated with plot number.

An average edaphic factor is calculated for each transect and presented in Table 2.

Table 2. Edaphic factors - average

Transect A	0.027
Transect B	0.026
Transect C	0.033

No significant difference in edaphic factor can be detected between transect A, B and C ($p\text{-value}_{\text{transect A-B}} = 0.86$; $p\text{-value}_{\text{transect B-C}} = 0.311$; $p\text{-value}_{\text{transect A-C}} = 0.13$).

3.2 Climatic components

3.2.1 Nt-factor

The nt-factor is calculated from NDVI by use of an empirical relation established from temperature data from mobile and fixed climate stations and corresponding NDVI values from mobile stations and Landsat 8. This relation is in accordance with a similar relation from Westermann et al. (2014) and thereby found to be acceptable (See paper ‘Estimating NDVI and nt-factor on Disko Island, Greenland, using different *in situ* methods’). The calculated nt-factors are presented in Figure 5.

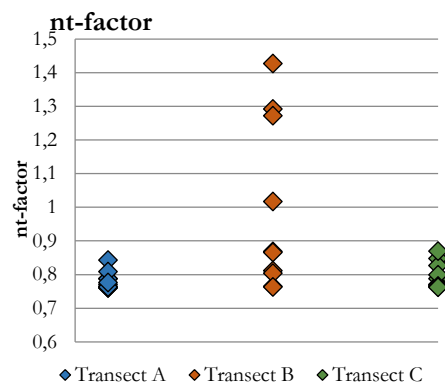


Figure 5. nt-factors for each plot, calculated from an empirical nt-NDVI relation.

Only small variations are seen for transect A and C, both fluctuating around an nt-factor of 0.8. Transect B experiences the largest differences between nt-factors for the 10 plots. This transect had the highest variability in surface cover, ranging from bare soil to vegetated. The majority of the plots have an nt-factor below 1, corresponding to higher air temperature than surface temperature.

3.2.2 Potential Radiation Index

The Potential Radiation Index (PRI) is calculated for the whole area of Blæsedalen and values for the three transects are extracted. Figure 6 shows the spatial distribution of PRI and values for each plot.

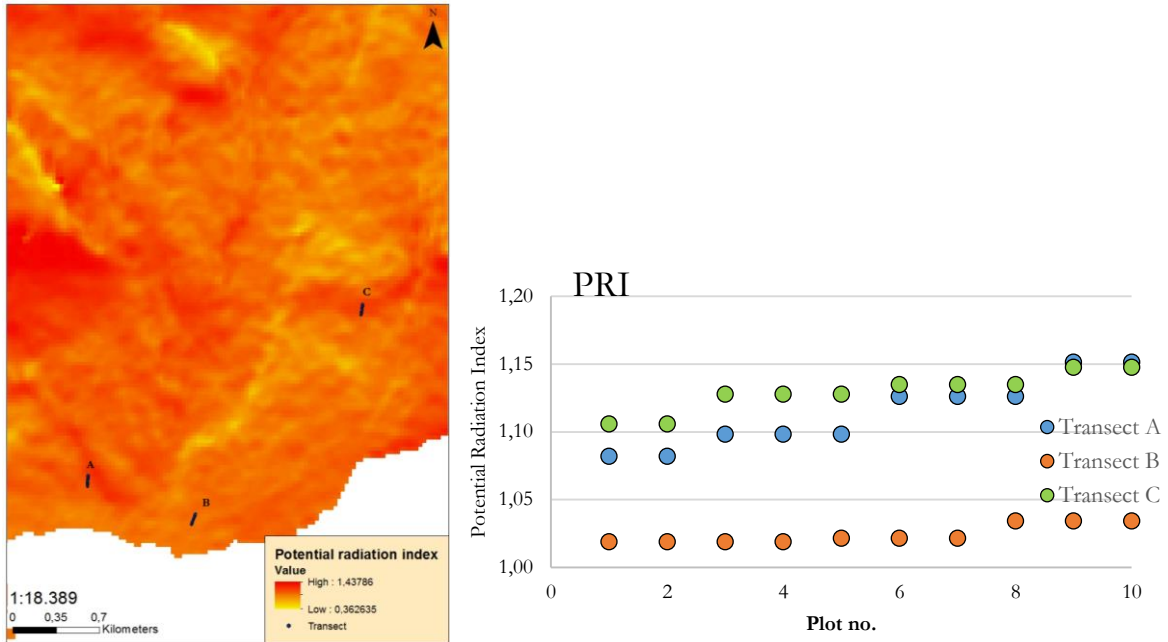


Figure 6. Potential Radiation Index for Blæsedalen (map) and transects.

The slope of the transects increased with increasing plot number, reflected in the values for potential radiation, which are all increasing with increasing plot number. All transects were south facing. Differences in PRI might therefore origin from small differences in slope, or in elevation. Transect A experiences the largest increase in PRI with plot number, corresponding to a large increase in slope with plot number. On average, Transect C has the highest PRI corresponding to having the highest elevation as well. Transect B experiences the lowest PRI and the least difference along the transect.

3.2.3 DDT

Degree Days of Thaw is presented for two consecutive years, 2013 and 2014, in Table 3.

Table 3. Degree Days of Thaw

Year	DDT (°C)
2013	834.4
2014	868.7

Degree Days of Thaw calculated as the sum of the average daily temperature above zero °C. Temperature data is from the fixed climate station at Østerlien. DDT has a large degree of similarity between the two years, and the value from 2014 will be used in calculation of active layers thickness.

3.3 Active layer thickness

Calculated active layer thickness for each transect is presented in Figure 7. Table 4 presents minimum and maximum as well as the range of calculated thicknesses for each transect.

Minimum values does not differ much between transects (maximum differences 0.07 m). However, maximum thickness between transects vary up to almost 0.30 m between transect C and B. The before seen patterns of transect B having the largest variations in several parameters are reflected in the active layer values, where Transect B has the largest difference in ALT between the plots.

In Stefan Solution, the climatic term is squared before multiplied with the edaphic factor. This indicates a perception of the edaphic factor as the controlling factor in estimating the active layer thickness. The edaphic factor for the 30 plots are evaluated to see if any clear correlation exists between edaphic factor and vegetation (represented by NDVI), water content or texture.

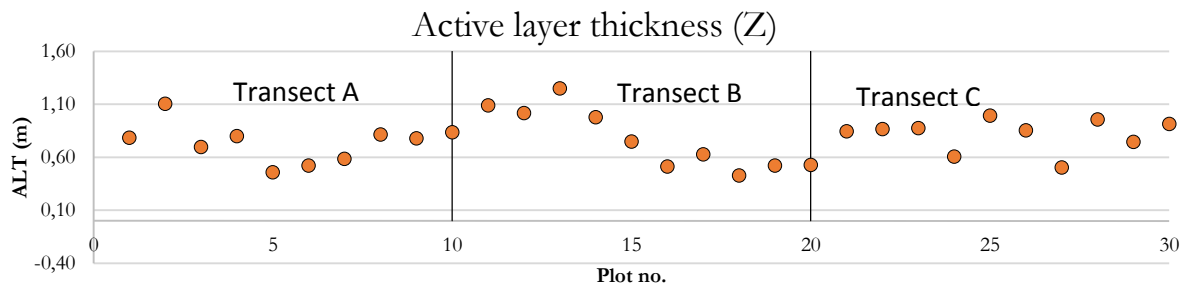


Figure 7. Active layer thickness

Table 4. Active layer thickness

	Average (m)	Minimum (m)	Maximum (m)	Span (m)
Transect A	0.74	0.46	1.10	0.65
Transect B	0.77	0.43	1.25	0.82
Transect C	0.81	0.50	0.99	0.49

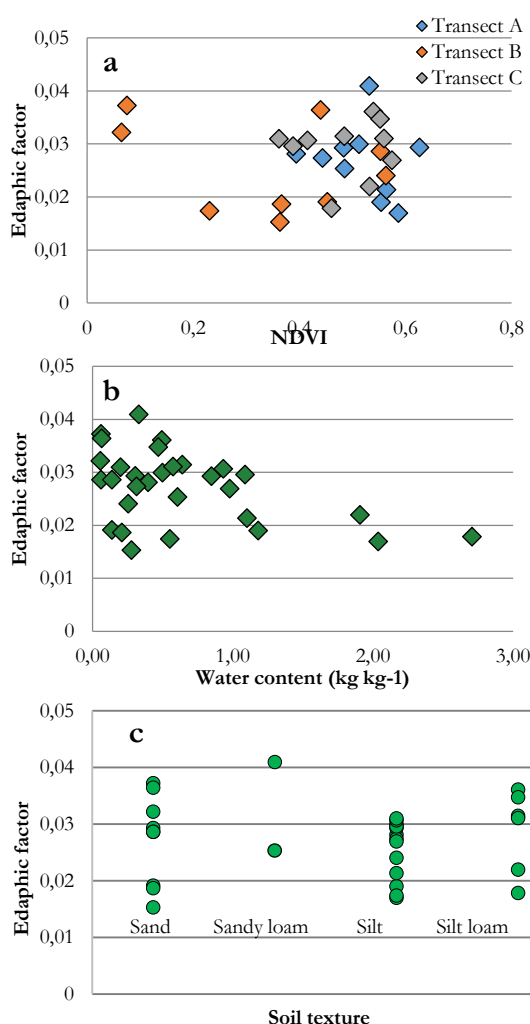


Figure 8. Edaphic factor as a function of NDVI (a), water content (b) and soil texture (c).

Figure 8 presents edaphic factor as a function of NDVI (a), water content (b) and texture (c).

No immediate correlation can be seen between NDVI and E, as both high and low NDVI experience high and low edaphic factors (Figure 8 a). Water content appears in the denominator in the edaphic factor equation (Equation 2) and lower edaphic factor with higher water content is thus expected. However, Figure 8(b) shows no significant relation between these two factors. The texture of the soil is determined from the particle size distribution. As seen from Figure 8(c) edaphic factor values are both high and low for each texture class, and there is no clear correlation between these two.

4. Discussion

Figure 7 presents calculated active layer thicknesses for each plot in the three transects. There were no clear trends in the active layer thickness within transect A and C. Transect B however, showed a trend of decreasing active layer thickness with increasing plot number. This correlates with a similar increase in vegetation cover and wetness, suggesting the active layer thickness decreases with increasing vegetation cover and wetness.

As differences in vegetation and wetness were the determining features in choosing the three locations, it was expected that these properties would be reflected in the active layer thickness calculations. Nonetheless, average thickness of the active layer does not vary as much between the three transects, neither does minimum nor maximum thicknesses,

despite a substantial difference in vegetation and wetness between the three transects.

Transect B deviated most from the other transects with respect to many of the input parameters. It had the lowest thermal conductivity, lowest water content, highest average bulk density, lowest PRI, and is the least vegetated. However, with respect to average edaphic factor and average active layer thickness, Transect B does not stand out compared to Transect A and C. Only within the transect, Transect B experiences a large difference in edaphic factor and active layer thickness.

Several factors can contribute to this absence of difference in estimated active layer thickness between transects. First of all, differences in vegetation and wetness could not be substantial enough due to overlap of plots between the transects with similar wetness and NDVI-values. Secondly, applied sampling strategy or assumptions made in ALT calculations could result in the absent difference in active layer thickness: the setup in the active layer thickness equation amplifies the edaphic factor in estimating the thickness over to the climatic components. Thus, incorrect values of edaphic factor due to e.g. methodological mistakes will influence active layer thicknesses more than incorrect values of the climatic components.

Calculated active layer thicknesses are compared to measured active layer thickness at Transect C where near-surface permafrost was observed. The thickness of the active layer was measured for plot 1-8 at Transect C and is about 2 to 3 times lower than what was calculated from Stefans Solution (see Table 5). Active layer thickness is thus overestimated for at least transect C, indicating overestimation of either the edaphic factor climatic components (DDT, nt-factor, PRI) or both.

Table 5. Estimated and observed active layer thicknesses for Transect C. Plot 9 and 10 are not shown as active layer thicknesses for these were not measured.

Plot	ALT estimated (m)	ALT observed (m)
C1	0.84	0.35
C2	0.86	0.40
C3	0.87	0.30
C4	0.60	0.20
C5	0.99	0.35
C6	0.85	0.65
C7	0.50	0.20
C8	0.95	0.36

4.1 Edaphic term

Since edaphic factor is a term characterizing the substrate's ability to support permafrost, it is very much reflected by the thermal properties of the soil, which again are highly influenced by water content and the organic-mineral composition of the soil. Overestimation of the edaphic factor might therefore origins from too high thermal conductivities or too low values for organic matter or water content.

Uncertainties regarding the performed ring sampling, such as presence of stones, roots and porous soil, all hindering the ring sample to reflect the exact conditions of the soil, are expected to only play a minor role in the ALT calculations. More critical is the measurements of thermal conductivities with the KD-2 pro Thermal Properties Instrument, as these show no clear dependency on water content or organic matter content. For instance, the thermal conductivity was generally measured lowest at Transect B even though water content and organic matter content were low as well. Several plots in Transect B had thermal conductivities measured between 0.13-0.14 W m⁻¹ K⁻¹, which are values corresponding to thermal conductivities of organic soils, even though the organic matter content was less than 2.5 %. If the KD-2 instrument did not produce reliable thermal conductivity values, this could influence the calculation of active layer thickness.

Table 6. ALT - Sensitivity to thermal conductivity ($\text{W m}^{-1} \text{K}^{-1}$) for Transect C.

	Average ALT (m)	Minimum (m)	Maximum (m)	Span (m)
Measured K (average 1.25)	0,81	0,50	0,99	0,49
Fixed K = 0.15	0,33	0,28	0,52	0,24
Fixed K = 3 W	1,49	1,24	2,33	1,09

In order to investigate the active layer thickness' sensitivity to thermal conductivities, fixed thermal conductivities are used for calculating the active layer thickness for transect C. Thermal conductivities for organic soil can be down to $0.15 \text{ W m}^{-1} \text{ K}^{-1}$ (Tritt, 2004). Furthermore, Westermann et al. (2014) describes a thermal conductivity up to $3.0 \text{ W m}^{-1} \text{ K}^{-1}$ for mineral soil, and this is applied as an upper limit. Table 6 shows the resulting active layer thicknesses.

The lower limit ($K=0.15 \text{ W m}^{-1} \text{ K}^{-1}$) results in thicknesses between 0.28-0.33 m, resembling measured thickness of 0.20-0.65 m much better than those calculated by Stefan's solution based on measured thermal conductivities. The upper limit ($K=3.0 \text{ W m}^{-1} \text{ K}^{-1}$) on the other hand, overestimate values even further. The calculation of the active layer thickness is highly sensitive to thermal conductivity, thus the reliability of the applied instrument is very important and inconsistent measurements given by the instrument can significantly affect active layer thickness calculations.

Besides instrumental uncertainties, the applied sampling strategy of soil samples and thermal conductivity could also cause unrealistic values of edaphic factor and active layer thickness. Soil samples and measurements of thermal conductivity were taken in the soil underneath the O-horizon. The O-horizon is an organic layer with lower thermal properties than the underlying soil (Bonnaveutre & Lamoureux, 2013).

Transect B had no or a very thin organic layer, whereas Transect C had a thick organic layer between 0.21-0.36 m. Transect A had an intermediate organic layer thickness. The effect of an organic layer is shown in Table 7, where the edaphic factor and active layer has been calculated for Transect C, assuming that the organic layer stretched down through the whole soil column.

As presented in Table 7, the thermal conductivities for the organic layer are significantly lower than thermal conductivities of soil.

With the assumptions that water content is the same as of the soil, and bulk density is 0.3 g/cm^3 as proposed by Campbell et al. (1994) for organic soils, the organic layer has a lower edaphic factor than the soil beneath. If the transect only consisted of an organic layer, the active layer thickness would be reduced by 0-0.30 m compared to estimated thicknesses. The active layer thickness would nonetheless still be overestimated compared to the measured thicknesses (see Table 5 for estimated ALT and measured ALT at Transect C). However, this calculation is based on the assumption that the water content of the organic layer was equal to the soil beneath. If the water content of the organic layer was higher than that of the soil, the active layer thickness of the organic layer would be lower than calculated here. On the other hand, the substrate of Transect C did not only consist of an organic layer and soil with higher thermal properties was present underneath. This would probably result in a smaller reduction of the active layer thickness than 0-0.30 m here estimated.

Table 7. Edaphic factor (EF) and active layer thickness (ALT) for the organic layer at Transect C is presented. The calculation of edaphic factor is based on measurements of thermal conductivity (TC) of the organic layer, and assumptions that the water content.

O-horisont (m)	TC (o-layer)	TC (soil)	EF (o-layer)	EF (soil)	ALT (o-layer, m)
Average	0.18	0.241	0.023	0.033	0.63
Minimum	0.15	0.092	0.008	0.018	0.22
Maximum	0.21	0.414	0.031	0.036	0.87

Thus, ignoring the presence of an organic layer does not seem to be the main reason for the overestimation of active layer thicknesses at Transect C.

Besides organic matter, thermal conductivity is also influenced by water content, and increases with soil water content (Breuning-Madsen, 2005). Field capacity and wilting point for the three transects are calculated and presented in Table 8 together with ALT for conditions at both field capacity and wilting point¹.

Table 8. Sensibility to soil water content. Grey highlights are measured values.

	A	B	C
Mean measured WC (%)	76.29	18.17	101.01
Mean WC at FC (%)	86.80	31.83	72.29
Mean WC at WP (%)	20.26	4.47	18.47
Mean measured ALT (m)	0.74	0.77	0.81
Mean ALT FC (m)	0.64	0.48	1.02
Mean ALT WP (m)	1.37	1.82	2.02
Differences(ALT_{WP}-ALT_{FC})	0.73	1.34	1

The table shows how Transect A is close to field capacity. Transect B is in between field capacity and wilting point. Transect C has a higher measured water content than field capacity, presumably due to the presence of permafrost that restricts drainage. Thus, ALT are higher at both field capacity and wilting point than measured values. Everything else being equal, the edaphic factor differs with different water content, in the order that the soils with water content at field capacity have lower edaphic factors than soils at wilting point. This difference in edaphic factor is reflected in the calculation of ALT, where active layer thicknesses are much smaller for wet soils at field capacity than for dry soils at wilting point.

In general, a validation of the in-situ measurement could have given an insight into whether or not the factors used had accurate results. Thermal conductivity had a high influence in the estimated ALT, and this could have been improved by using another method beside the chosen in-situ measurement.

¹ Calculated after Breuning-Madsen & Krogh (2005).

Water content in the soil will change over time, and the chosen method gave a time specific measure of how the soil was saturated. Table 8 shows that this could have an important impact on the ALT, and a more thorough investigation could illustrate the changes water contents influence on ALT.

4.2 Climatic term

The climatic term is highly influenced by temperature and potential critical sources of error therefore very much related to collection of temperature data.

The Degree Days of Thaw used as input in Stefan's solution might cause active layer thicknesses to be overestimated for especially Transect B and C. Transect B and C are located at the mouth of Blæsedalen and inside of Blæsedalen, respectively. However, climate data is obtained from the fixed climate station located in Østerlien. Inland-coastal as well as elevation climate gradients might alter air temperatures and therefore result in much different DDT between these locations. Comparison of annual air temperatures from the fixed climate stations at Østerlien and Blæsedalen shows how Blæsedalen in general experiences cooler air temperatures than Østerlien. Thus, lower DDT at transect B and C than at transect A is expected. DDT is calculated for 2014 based on temperature data from the fixed climate station at Blæsedalen. For this particular year, DDT differentiates with 102 degree days between Østerlien and Blæsedalen ($DDT_{Østerlien}=869$; $DDT_{Blæsedalen}=767$). Resulting differences in active layer thickness are shown in Figure 9.

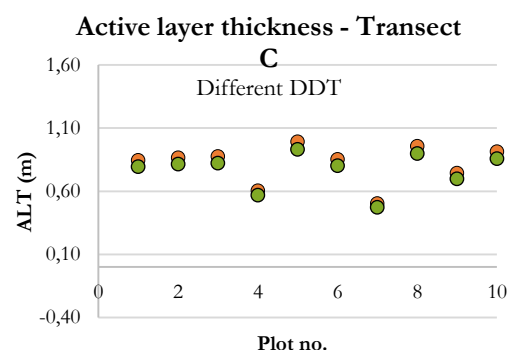


Figure 9. Active layer thickness by use of different DDT based on temperature data from Østerlien (red) and Blæsedalen (green).

Active layer thickness is slightly smaller with use of DDT from Blæsedalen than Østerlien (average difference is 0.05 m).

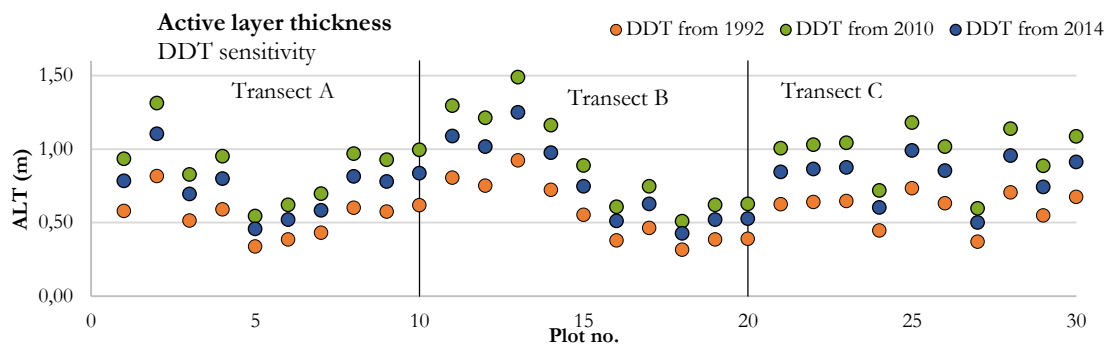


Figure 10. Active layer thickness by use of different DDT (coolest year 1992, warmest year 2010).

However, actual DDT at transect C might be even lower due to the higher elevation and the location further into Blæsedalen.

Difference in elevation between transects and climate stations from where DDT is obtained might cause a difference between air temperatures that can be accounted for by incorporating a theoretical or empirical lapse rate. The temperature sensor at the climate station in Blæsedalen is located 99.2 m above sea level whereas the sensor at Østerlien is 28.1 m above sea level. Transect A, B and C have average elevations of 52.3, 47.2, and 117.4 m above sea level, respectively. Fausto et al. (2009) estimated the mean monthly slope lapse rates for the summer months (June, July, August) to be an average of 0.50 °C per 100 m, based on calculations between stations along seven different transects around Greenland. As an example, the difference between elevations at transect A and climate station Østerlien is 24.2 m, thus corresponding to a theoretical summer temperature difference of 0.12 °C. DDT for Østerlien 2014 is adjusted to account for this, resulting in only a small lowering of DDT from 859 to 841 degree days. Thus, elevation differences between transects and climate stations only plays a minor role in DDT and active layer calculations.

The close proximity to the coast for transect B is expected to impact temperatures and thus DDT. According to Rouse (1991), cold air masses from the sea can impose cold air temperatures of adjacent terrestrial environments. A gradient of cooler temperatures closer to the coast might therefore exist, resulting in even lower DDT at transect B than further inland.

Inter-annual variations in air temperature might influence modelled active layer thickness. DDT is calculated for 2013-2014 and does not vary much between those two years. However, the actual value for 2015 might prove to be different.

In order to investigate this possible difference, temperature time series from 1991-2015 from a fixed climate station at the scientific leaders house next to arctic station has been analysed. Degree days for the coolest (1992) and warmest year (2010) is calculated and varies with a maximum of 758 degrees days. Figure 10 presents active layer thickness modelled with DDT from 1992, 2010, and 2014, all other factors being equal.

Active layer thickness varies with an average of 0.35 m between the coolest and warmest year in the analysed time series. However, temperature is related to PRI, nt and water content, factors being held constant in the above presented results. Those factors are different under different temperature conditions and might influence the active layer calculations and thus alter the above presented patterns. Figure 10 illustrates how ALT depends on DDT, and how DDT changes noteworthy between years. Different climatic inputs for the different study sites could have resulted in a more influential climatic factor on ALT.

The nt-factors estimated for the three transects is based on an established nt-NDVI relation (see paper ‘Estimating NDVI and nt-factor on Disko Island, Greenland, using different in situ methods’). As discussed in the article several assumptions have been made in order to establish this relation. These include interpolation of temperature data from one location to apply for other areas and applying NDVI values from the middle of the day when the temperatures are highest. Westermann et al. (2014) also present

an nt-NDVI relation. This nt-NDVI relation generates lower nt-factor values than by use of the present established nt-NDVI relation. The effect of this difference between nt-NDVI relations is shown in Figure 11.

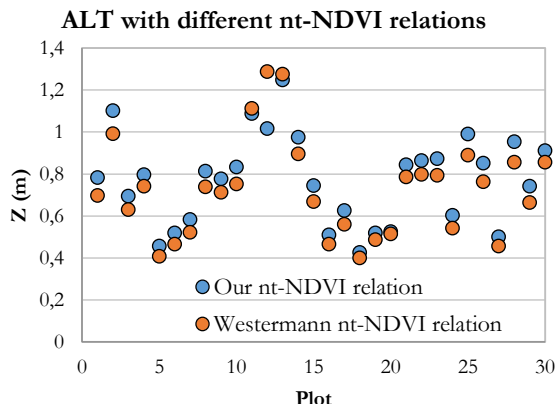


Figure 11. Active layer thicknesses (ALT) for nt calculated by our nt-NDVI relation compared to nt-factors calculated based on nt-NDVI relation established by Westermann et al. (2014).

The lower nt-factors of Westermann et al. (2014) result in slightly lower active layer thicknesses. However, with an average difference of 0.05 m in active layer thicknesses between nt-factors obtained from our relation compared to Westermann et al. (2014), the thicknesses are still overestimated.

The methodological choices and assumptions made influence active layer thickness. Sensitivity of the model to the different input factors (thermal conductivity, DDT, nt-factor, water content) is evaluated and each component effects the calculated thicknesses in different ways. It is important to consider that most factors are related to each other in ways that make tuning of only one component at a time less realistic.

Stefan Solution and its modifications are the most widely employed equation in active layer modelling and thereby well tested (Riseborough, et al., 2008). However, with all modelling, model accuracy is to a great extent dependent on which and how many processes are included, as well as the data available. Stefan's solution is often applied on a regional scale (Riseborough, et al., 2008), but has in this article been applied on a small scale investigating active layer thickness for three 100 m transects.

5. Conclusion

Stefans Solution has been applied on three transects in and around Blæsedalen, resulting in active layer thicknesses of 0.74, 0.77 and 0.81 m (average values) for transect A, B and C. Measurements of active layer thickness at Transect C, where near-surface permafrost was observed, show thicknesses about 2 to 3 times lower than what was estimated. Thus, Stefan Solution seems to overestimate the depth of permafrost on Transect C.

The sensitivity of modelled active layer thickness has been investigated with respect to thermal conductivity, water content, Degree Days of Thaw and nt-factor. Active layer thicknesses proved to be highly sensitive to thermal conductivity, highlighting the importance of reliable methods of measurements. Active layer thickness with water content at field capacity and wilting point also showed large differences in active layer thicknesses (up to 1.34 m) between those two extremes.

Different values of DDT had a notable influence on modelled active layer thickness. DDT varies with coastal-inland and elevation gradients as well as between years, and using the correct input of DDT is therefore fundamental in estimating active layer thickness correct. On the other hand, using different NDVI-nt relations in determining the nt-factors had no noteworthy influence on active layer thicknesses.

6. Literature

- Bonan, G., 2008. *Ecological Climatology - Concepts and Applications*. 2. ed. New York: Cambridge University Press.
- Bonnaventure, P. P. & Lamoureux, S. F., 2013. The active layer: A conceptual review of monitoring, modelling techniques and changes in a warming climate. *Progress in Physical Geography*, 37(3), pp. 352-376.
- Breuning-Madsen, H. & K. L., 2005. *Kompendium i jordbundsgeografi*. Copenhagen: Geografisk Institut, Københavns Universitet.
- Campbell, G. S., Jungbauer, J. D., Bidlake, W. R. & D., H. R., 1994. Predicting the effect of temperature on soil thermal regimes. *Soil science*.
- Decagon Devices, Inc., 2015. *KD2 Pro Thermal Properties Analyzer - Operator's Manual*, Pullman: Decagon Devices, Inc..
- Edwards, J., Wood, C. W., Thurlow, D. L. & Ruf, M. E., 1999. *Total Organic Carbon*. [Online] Available at: http://soilquality.org/indicators/total_organic_carbon.html [Senest hentet eller vist den 27. 10. 2015].
- Elberling, B., Jakobsen, B. H., Søndergaard, J. & Sigsgaard, C., 2004. *Influence of Vegetation, Temperature, and Water Content on Soil Carbon Distribution and Mineralization in four High Arctic Soils*. s.l.:Arctic, Antarctic, and Alpine Research, Vol. 36, No..
- ESRI, 2012. *How solar radiation is calculated*. [Online] Available at: http://resources.arcgis.com/EN/HELP/MAIN/10.1/index.html#/How_solar_radiation_is_calculated/009z000000tm000000/.
- Fausto, R. S. A. A. P. & V. A., 2009. A new present-day temperature parameterization for Greenland.. *Journal of Glaciology*, Vol. 55, No. 189.
- Karlsen, S. R. et al., 2008. MODIS-NDVI-based mapping of the length of the growing season in northern Fennoscandia. *International Journal of Applied Earth Observation and Geoinformation*, pp. 253-266.
- Klene, A. E., Nelson, F. E. & Shiklomanov, N. I., 2001. The N-factor in Natural Landscaped: Variability of Air and Soil-Surface Temperatures, Kuparuk River Basin, Alaska, U.S.A.. *Arctic, Antarctic, and Alpine Research*, 33(2), pp. 140-148.
- Mariager, T. & N. E. L., 2014. Edaphic factor of soils in Blæsedalen, Disko Island - A pedological study of the abiotic factors controlling the edaphic factor.. *University of Copenhagen, Field and Methods Course – Greenland..*
- Nelson, F. E.; Shiklomanov, N. I.; Mueller, G. R.; Hinkel, K. M.; Walker, D. A.; Bockheim, J. G., 1997. Estimating Active-Layer Thickness over a Large Region: Kuparuk River Basin, Alaska, U.S.. *Arctic and Alpine Research*, Vol. 29(No. 4), pp. 367-378.
- Nelson, F. E. & Outcalt, S. I., 1987. A Computational Method for Prediction and Regionalization of Permafrost. *Arctic and Alpine Research*, 19(3), pp. 279-288.
- Pennock, D., Yates, T. & Braidek, J., 2008. Soil Sampling Designs. I: M. Carter & E. Gregorich, red. *Soil Sampling and Methods of Analysis*. s.l.:Canadian Society of Soil Science, pp. 1-14.
- Polar Science Center, 2010. *Collaborative Research: The Impact of Arctic Storms on Landfast Ice Variations*. [Online] Available at: http://psc.apl.washington.edu/nonwp_projects/landfast_ice/freezing.php [Senest hentet eller vist den 26. 10. 2015].
- Riseborough, D. et al., 2008. Recent Advances in Permafrost Modelling. *Permafrost and Periglacial Processes*, Issue 19, pp. 137-156.
- Rouse, W. R., 1991. Impacts of Hudson Bay on the Terrestrial Climate.. *Arctic and Alpine Research*, Vol. 23, No. 1, pp. 24-30.
- Tritt, T. M., 2004. *Thermal conductivity Theory, Properties and Applications..* New York: Plenum.
- Westermann, S. et al., 2014. Future permafrost conditions along environmental gradients in Zackenberg, Greenland. *The Cryosphere*, Issue 9, pp. 719-735.
- Zhang, T. et al., 2005. Spatial and temporal variability in active layer thickness over the Russian Arctic drainage basin. *JOURNAL OF GEOPHYSICAL RESEARCH*, Årgang 110, p. D16101.

Appendix 1. Field schedule

Date	
2 nd of August 2015	Arrival at Arctic Station in the evening
3 rd of August 2015	Introduction to Arctic station and Blæsedalen Initial test of instruments, visiting Østerlien, snow fence site in Blæsedalen and the area around transect 3 (lake). Introduction to fixed climate stations.
4 th of August 2015	Measurements at transect 1: Østerlien. Establishing transect from South to North. Measurement of NDVI by Skye sensor and camera, soil moisture, thermal conductivity, cover fraction analysis, surface temperature, incoming solar radiation, soil samples.
5 th of August 2015	Measurements at transect 2: Abrasionplate Establishing transect from South to North. Measurement of NDVI by Skye sensor and camera, soil moisture, thermal conductivity, cover fraction analysis, surface temperature, incoming solar radiation, soil samples. Preparing of transect 3 at Lak. Weighting of soil samples.
6 th of August 2015	Measurements at transect 3: Lake Measurement of NDVI by Skye sensor and camera, soil moisture, thermal conductivity, cover fraction analysis, surface temperature, incoming solar radiation, soil samples.
7 th of August 2015	CALM Site Permafrost measurements for 100 plots in the CALM site grid, using probe. NDVI measured by Skye sensor for each point.
8 th of August 2015	Data processing Analysis of NDVI camera pictures. Weighting and drying of soil samples.
9 th of August 2015	Data processing NDVI camera pictures, vegetation cover. Weighting and drying of soil samples. Collecting of NDVI via Decagon, Skye and camera for 25 additional points (later dismissed).
10 th of August 2015	Additional NDVI points Collecting of NDVI via Decagon, Skye and camera for 35 randomly distributed additional points.
11 th of August 2015	Data processing Initial establishment of relations between Skye, Decagon and camera NDVI. Thermal conductivity measured again at Transect 1 plots.
12 th of August 2015	Leaving Arctic Station